Chapter 7

Nuclear Magnetic Resonance Spectroscopy for Structural Characterization of Bioactive Compounds

Clementina M.M. Santos[1] and Artur M.S. Silva[2]
[1]*Department of Vegetal Production and Technology, School of Agriculture, Polytechnic Institute of Bragança, Bragança, Portugal*
[2]*Department of Chemistry & QOPNA, University of Aveiro, Aveiro, Portugal*

Contents

7.1 INTRODUCTION

The structural assignment of a new natural product molecule is not only to establish the 3D structure of a compound, but potentially to provide the basis for research in a multitude of disciplines, ultimately generating new therapeutic agents and/or new understanding of disease biology. The development of modern spectroscopic techniques has transformed the structure assignment process, which previously was essentially based on chemical degradation or derivatization followed by partial or total synthesis. Notably, it was only in the specialization era of the spectroscopic structural assignment of natural products that the field of marine natural products chemistry took shape.

Today the processes of marine and terrestrial natural product isolation and structural determination are frequently streamlined and expeditious due to the

Analysis of Marine Samples in Search of Bioactive Compounds, Vol. 65. DOI: 10.1016/B978-0-444-63359-0.00007-0

spectacular advances in chromatographic and spectroscopic technologies as well as chemical synthesis.

The NMR spectroscopy is a powerful tool in structure elucidation because the properties it displays can be related to the molecular structure. The chemical environment of a particular nucleus is associated with the *chemical shift* (δ, ppm), and the *area* of a resonance, usually presented as its relative integral, is related to the number of nuclei giving rise to the NMR signal. The interactions between individual nuclei, mediated by electrons in a chemical bond, determine the *coupling constant* (J, Hz). In this chapter we will present the techniques commonly used, basic concepts, and how they are useful for chemists in the structural elucidation of mainly bioactive marine natural products. Its complex planar structure is determined by ^{1}H and ^{13}C NMR analysis strongly supported by other 1D (DEPT) and 2D (COSY, TOCSY, HSQC/HMQC, HMBC) NMR techniques. The stereochemistry is generally based on NOE experiments (NOE difference, NOESY, and ROESY), ^{1}H–^{1}H and ^{1}H–^{13}C coupling constants, chiral derivatizing agents, and also in empirical procedures comparing the chemical shifts of unknown vicinal and proximal centers with libraries of configurationally known stereomodels. However, the most reliable option to assign all the 3D structure of a marine natural product still is their total synthesis.

The use of NMR hyphenated with other chromatographic and spectroscopic techniques and microcoil probes and narrow diameter tube probes for the structural elucidation of bioactive marine natural products, mainly associated with the quantitative NMR determinations, will be also briefly described.

The chapter will finish with a description of the structural characterization of several types of marine natural products using all the referred NMR techniques followed by a small reference to the misassignments that still are very common.

7.2 PROTON RESONANCES ASSIGNMENT

The ^{1}H NMR spectra of marine natural products are generally very complicated since their structures generally possess a great number of aliphatic and/or aromatic carbons. For example, the polyoxy linear carbon chain of prorocentrol **1**, a potential cytotoxic and antidiatom agent, presents 75 proton resonances in a range of 0.89 to 6.52 ppm (aliphatic and olefinic protons) [1] and the *O*-sulfated pyrrole alkaloid baculiferin B **2** presents 12 proton resonances in a small range of the aromatic region 6.35 to 7.85 ppm [2]. However, there is also some simple ^{1}H NMR spectra, due to the structure simplicity (e.g., bromopyrrole sulfonic acid **3** [3]) or symmetry (e.g., chrysazin **4** [4]; Figure 7.1).

In the case of complex NMR spectra, it is necessary to use some ^{1}H–^{1}H correlated 2D NMR techniques to help in the assignment of all the proton resonances. One of these techniques is the ^{1}H–^{1}H COSY (COrrelation SpectroscopY) spectrum, which simply identifies protons that are coupled with each other. In this technique, 1D spectrum is displayed along each axis with a contour projection of this spectrum along the diagonal axis. Off-diagonal peaks represent

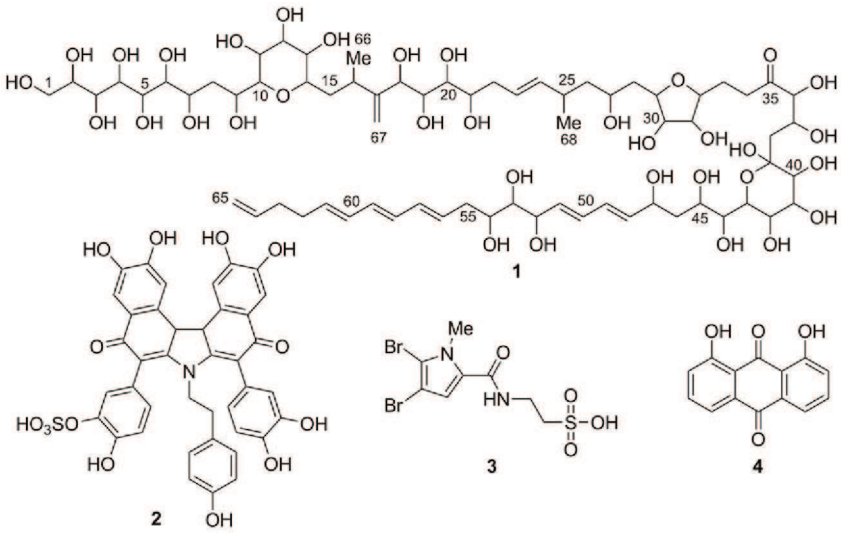

FIGURE 7.1 Structures of compounds **1–4**.

proton shift correlations (or proton couplings). The COSY correlations allow the establishment of some structure moieties, which combined with heteronuclear ^{1}H-^{13}C NMR connectivities, allowed the assignment of all proton resonances and the full structure elucidation. This was the case of the antifungal neomaclafungin A **5** [5] and of the anticholinesterase inhibitor geranylphenazinediol **6** [6] (Figure 7.2). Specifically, the COSY spectrum of geranylphenazinediol **6** showed that protons H-2 (7.17 ppm) and H-3 (7.61 ppm) are coupled with each other (J 7.7 Hz) and the long range correlation of H-3 to the methylenic group H-1′ confirm the attachment site of the geranyl substituent. Vicinal and long range correlations of this chain of protons starting from H-1′ allows their complete assignment (Figure 7.2). The protons sequence H-7 to H-9 of the

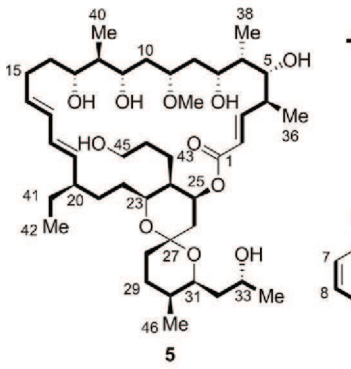

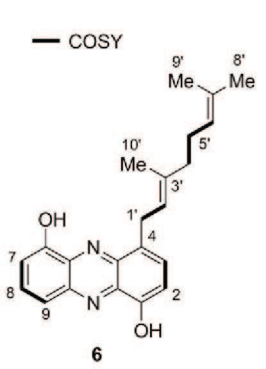

Compound **6**

	δ_H (ppm)	COSY
H-2	7.17, d	3
H-3	7.61, dt	2, 1'
H-7	7.25, dd	8, 9
H-8	7.82, dd	7, 9
H-9	7.73 dd	7, 8
H-1'	4.05, br d	3, 2', 4',10'
H-2'	5.54, tq	1', 4', 10'
H-4'	2.10, m	1', 2', 5'
H-5'	2.13, m	4', 6', 8', 9'
H-6'	5.10, tsept	5', 8', 9'
H-8'	1.59, br s	5', 6'
H-9'	1.55, br s	5', 6'
H-10'	1.80, br s	1', 2'

FIGURE 7.2 COSY correlations of neomaclafungin A **5** and geranylphenazinediol **6**.

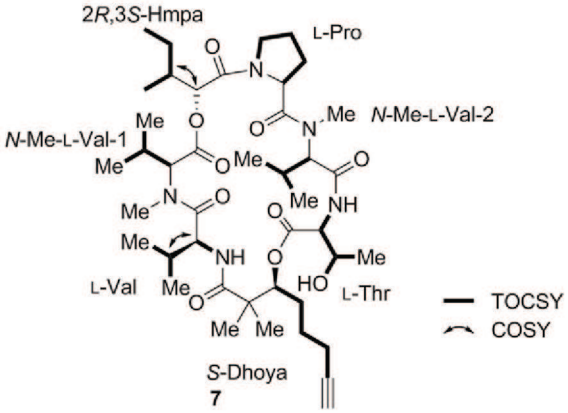

FIGURE 7.3 TOCSY and COSY correlations of viequeamide A **7**.

second aromatic ring of phenazine is also established by the COSY correlations of H-7 (7.25 ppm, dd, *J* 7.7, and 1.0 Hz) with H-8 (7.82, dd, *J* 8.9, and 7.7 Hz) and H-9 (7.73, dd, *J* 8.9 and 1.0 Hz), and also H-8 with H-7 and H-9. Then, the full structure elucidation needed information from the ^{13}C NMR data.

TOCSY (TOtal Correlation SpectroscopY) or HOHAHA (HOmonuclear HArtmann-HAhn) spectrum is another technique used to resolve complex proton NMR spectra. It presents correlations between all the protons within a given spin system, irrespective of whether they are directly coupled or not. For example, the TOCSY experiment of viequeamide A **7**, a cytotoxic agent of H460 human lung cancer cell lines, revealed eight proton spin systems (Figure 7.3). Four of them were assigned to the amino acid residues threonine (L-Thr), proline (L-Pro), and two *N*-methylvaline (*N*-Me-L-Val) units [7]. Two other spin systems were connected by COSY, which suggests that a possible constrained rotation might prevent strong TOCSY correlations within this residue. Heteronuclear correlations confirmed that these two spin systems belong to a valine residue (L-Val) wherein a very small $J_{H\text{-}\alpha,H\text{-}\beta}$ 2.3 Hz was present. The third unassigned and very weak TOCSY spin system was revealed by a combination of homo- and heteronuclear correlations as the hydroxy acid analogue of isoleucine (2*R*,3*S*-Hmpa). The remaining TOCSY spin system was characteristic of a polyketide synthase-derived residue, defined as a derivative of 2,2-dimethyl-3-hydroxy-7-octynoic acid (*S*-Dhoya) based on the long range ^{1}H-^{13}C connectivities. This type of connectivities together with ROESY data (see Section 7.4) allowed the establishment of the sequence of residues of viequeamide A **7**.

A variant of the COSY technique, the phase-sensitive DQF-COSY (Double Quantum Filtered-COrrelated SpectroscopY), is sometimes used to simplify the diagonal of the COSY spectrum and also to eliminate the singlets of this diagonal. The combination of this spectrum with a TOCSY spectrum elucidates partial substructures of prorocentrol **1**: H-1 to H-16, H-18 to H-34, H-36 to H-38, H-40 to H-65 [1] (Figure 7.4).

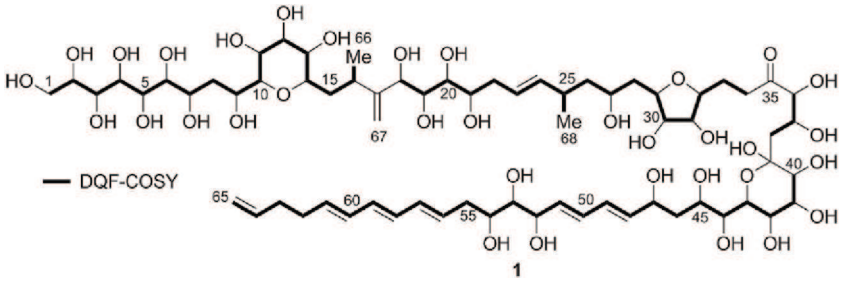

FIGURE 7.4 DQF-COSY correlations of prorocentrol **1**.

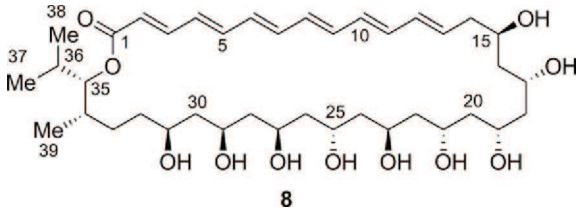

FIGURE 7.5 Structure of bahamaolide A **8**.

A general problem that can also appear in the ^{1}H NMR spectra of complex marine products are the overlapping of proton signals with that of the solvent. A possible way to circumvent this problem is to change the NMR solvent [8]. For example, in the ^{1}H NMR spectrum of a pyridine-d_5 solution of the antifungal bahamaolide A **8** (Figure 7.5), a 36-membered macrocyclic lactone, the carbinol resonances are well separated and easily assigned while olefinic signals overlap significantly with the solvent. Changing the solvent for CD_3OD, the alkene protons were well separated and the large vicinal ^{1}H-^{1}H coupling constants (J 14.5–15.5 Hz) allowed assignment of the (*E*)-configuration for all double bonds [9].

In many samples, OH and NH resonances can be recognized by their characteristic chemical shifts or broadened appearance in the ^{1}H NMR spectrum but they vary depending on the sample preparation, product structure, and ability to form hydrogen bonds. Higher chemical shifts are observed in samples with higher product concentration (increased hydrogen bonding), in H-bonded groups compared to free OH or NH groups, and in H-bonding solvents like DMSO-d_6 or acetone-d_6.

OH and NH resonances are subject to intermolecular exchange processes in some solvents, which may result in broadening or complete loss of coupling with neighboring protons. As example of the last phenomena, the signals of the six hydroxyl groups (δ 9.41–10.10 ppm) in the ^{1}H NMR spectrum of the potential antibiotic agent chrysophaentin A **9** in DMF-d_7 were completely absent in the spectra recorded in $CDCl_3$, CD_3CN, and DMSO-d_6 [10]. The broad singlets attributed to the OH and NH protons in the ^{1}H NMR spectra of the antifungal ambiguine P **10** and the antibacterial ambiguine Q nitrile **11** acquired in DMSO-d_6

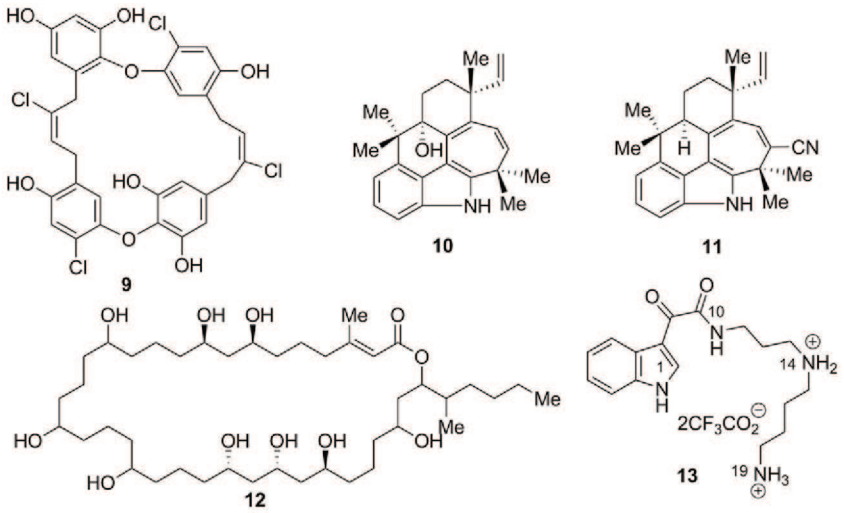

FIGURE 7.6 Structures of compounds **9–13**.

are completely absent in the spectra recorded in CD_3OD at 900 MHz [11]. The ^1H NMR spectra of the macrolactone caylobolide B **12**, a cytotoxic agent against HT29 colorectal adenocarcinoma and HeLa carcinoma cell lines, presented nine OH exchangeable protons at 4.20 to 4.52 ppm [12], and that of the antimicrobial indole spermidine alkaloid didemnidine A **13** exhibited seven exchangeable protons assigned to the NH resonances: indole NH-1 at 12.29 ppm, secondary amine NH-10 at 8.90 ppm, protonated secondary amine NH_2-14 at 8.54 ppm, and finally protonated primary amine NH_3-19 at 7.81 ppm [13] (Figure 7.6).

The rates of exchange are strongly dependent on the temperature, solvent, concentration, and presence of acidic and basic impurities. In $CDCl_3$, the presence of acidic impurities (usually from solvent decomposition) leads to rapid acid-catalyzed exchange between H-bonded groups. In solvents like DMSO-d_6 and acetone-d_6 the strong hydrogen bonds of the H-bonded groups slows down the intermolecular proton exchanges, leading to discrete OH or NH signals with observable coupling to nearby protons.

In some cases the disappearance of all OH and NH signals can be useful. For that, the labile protons can be easily identified by shaking the sample with a drop of D_2O. This process present better effects if the solvent is water immiscible and denser than water ($CDCl_3$, CD_2Cl_2, CCl_4) since the formed DOH is in the drop of water floating at the top of the sample where it is not detected. In water miscible solvents (acetone-d_6, DMSO-d_6, CD_3CN, pyridine-d_5, THF-d_8) the OH and NH signals are converted to OD and ND, but the DOH formed remains in solution and appears in the water region.

Changing solvents can be a problem in terms of structure elucidation, since the use of deuterated protic solvents can give rise to the labeling of some exchangeable protons in the target molecule. Thus changing $CDCl_3$ for CD_3OD,

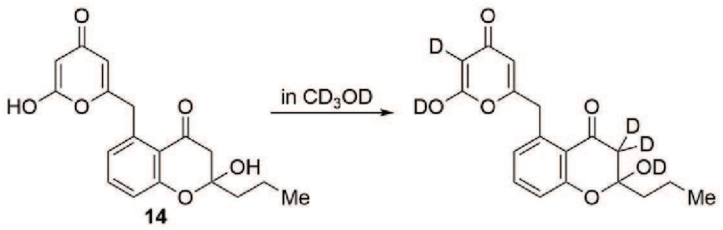

SCHEME 7.1 Deuteration of the antibacterial marine chroman-4-one **14** in CD_3OD.

the ^1H NMR spectrum of the antibacterial marine chroman-4-one **14** showed a fast disappearance of three signals corresponding to an olefinic proton, as a singlet at 5.33 ppm, and two methylene protons, as doublets at 2.79 and 2.89 ppm, due to tautomeric equilibria (Scheme 7.1). The incorporation of five deuterium atoms (the previously described plus the OD groups) was confirmed by ESI(+)-MS [14].

7.3 ESTABLISHMENT OF CARBON SKELETON

Similar to ^1H NMR spectroscopy, ^{13}C NMR of biologically active marine natural products can also be very complex. For instance, the spectrum of prorocentrol **1** (Figure 7.4), a polyoxy linear compound presents 67 carbon resonances in a range of 21.4 and 136.9 ppm plus the carbonyl carbon at 213.0 ppm. The signals around the acetal and carbonyl groups split in two or three signals, probably due to reversible formation of an acetal ring when measured in CD_3OD or DMF-d_7. This situation was not solved even by varying the NMR conditions such as solvents, temperature, and pH, but in a mixture of pyridine-d_5/D_2O (6:1) at room temperature the spectrum was simplified and improved, being the referred signals observed as a single peak each in the ^{13}C NMR spectrum [1].

The first attempt to assign the signals of complicated ^{13}C NMR spectra is through DEPT (Distortionless Enhancement by Polarization Transfer) experiments, which provide information about the nature of carbon atoms (distinguishing among ^{13}C signals of methyl, methylene, and methine carbons). Three DEPT spectra are required for a full analysis and use a complex series of pulses in both the ^1H and ^{13}C ranges: a 45° pulse (DEPT-45) in which all H-bearing carbon peaks are positive, a 90° pulse (DEPT-90) where only methine carbons are seen, and a 135° pulse (DEPT-135) where methyl and methine carbons present positive signals and methylene carbons give negative signals. Quaternary carbons are not seen in DEPT spectra because the technique relies on polarization transfer, which in this case is the transfer of proton magnetization onto the directly bound carbon atoms. In the ^{13}C NMR spectrum of bahamaolide A **8**, where a great number of signals appears in very small ranges of chemical shifts, the DEPT spectra assigned the carbon signals into one quaternary carbon

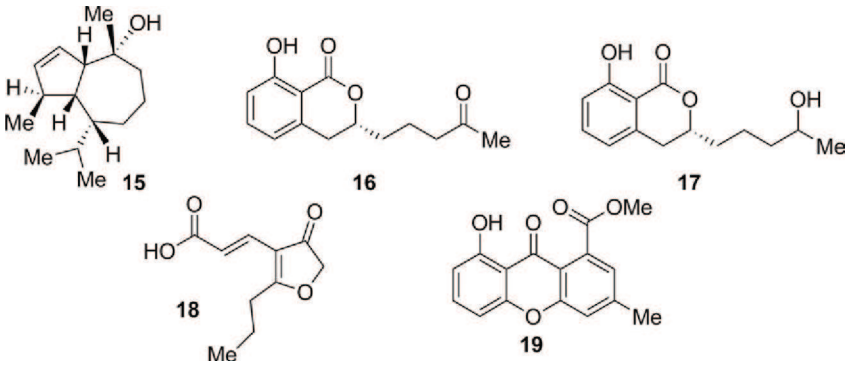

FIGURE 7.7 Structures of compounds **15–19**.

(168.0 ppm), 12 olefinic methines (121.1–146.0 ppm), 10 oxygenated methines (65.0–79.3 ppm), 12 aliphatic methylenes (30.9–48.3 ppm), one aliphatic methine (30.2 ppm), and three methyls (14.9–20.6 ppm) [9]. For a guaiane sesquiterpene derivative **15** where the ranges of some different types of carbons are overlapped, the DEPT spectra were very important to assign their 15 carbon resonances, appearing between 18.8 and 134.5 ppm, as two olefinic methines (132.9–134.5 ppm), one oxy quaternary carbon (73.4 ppm), five aliphatic methines (33.5–49.4 ppm), three methylenes (18.8–38.2 ppm), and four methyls (19.5–26.3 ppm) [15] (Figure 7.7).

The DEPT NMR spectra can also be very useful to assign the type of carbons in molecules bearing aromatic, aliphatic, and/or olefinic moieties. For example, in one of the dihydroisocoumarins isolated from endophytic fungus *Aspergillus* sp. (compound **16**), we can find five quaternary carbon atoms (108.2–208.2 ppm), including one lactone carbonyl carbon (169.7 ppm) and one ketone carbonyl carbon (208.2 ppm), three aromatic methines (116.0–136.1 ppm), one aliphatic oxymethine (79.3 ppm), four methylenes (18.9–42.7 ppm), and one methyl (29.8 ppm). The main difference for the second derivative (compound **17**) was the absence of the ketone carbonyl atom and the appearance of an aliphatic oxymethine at 67.3 ppm [16] (Figure 7.7). Compounds **16** and **17** presented a weak antibacterial activity against *Staphylococcus aureus* and *Bacillus subtilis*.

Cillifuranone **18**, a natural antibiotic compound produced by a fungal isolate from *Tethya aurantium*, presents 10 signals assigned as three carbonyl or enol carbons (170.9, 196.7, and 201.7 ppm), two olefinic methines (118.5 and 133.0 ppm), one quaternary olefinic carbon (112.6 ppm), one oxymethylene (76.3 ppm), two methylenes (20.9 and 31.6 ppm), and one methyl (14.0 ppm) based on DEPT spectra [17] (Figure 7.7).

In the case of the new antifungal marine xanthone derivative **19** the information given by the DEPT spectra is not very relevant since from their 16 signals, five are aromatic methines, nine are quaternary carbons, and two are methyl

groups [18] (Figure 7.7). The structure elucidation of many other marine products involved the use of this 1D NMR technique [3,9,19–21].

For routine work, similar information is obtained from HSQC (Heteronuclear Single Quantum Correlation) and HMQC (Heteronuclear Multiple Quantum Coherence) experiments. These two techniques provide single bond heteronuclear shift correlation, identifying one-bond H–C connectivities within a molecule. The 2D spectrum displays in one dimension ^{1}H chemical shifts and the other ^{13}C chemical shifts and the cross-peaks in the contour plot define to which carbon a particular proton (or group of protons) is directly attached.

HMBC (Heteronuclear Multiple Bond Correlation) is an extremely powerful tool in structure elucidation of marine natural compounds. This experiment establishes the long-range ^{1}H–^{13}C correlations, which typically occur over two and three bonds ($^{2,3}J_{C\text{-}H}$ usually < 10 Hz). Correlations can also be observed to quaternary centers (for example in the assignment of carbonyl resonances) and across heteroatoms other than carbon (for example hydroxyl protons).

These heteronuclear correlation spectra cannot be used alone; they are always combined and analyzed after ^{1}H assignment of a certain molecule. For instance, in the case of trichoderone **20**, a cytotoxic agent isolated from the marine fungus *Trichoderma* sp., the ^{1}H, ^{13}C, and HMQC spectra indicate the presence of two oxygenated methines [δ_C 77.7 (d, C-4) and 81.8 (d, C-5); δ_H 4.66 (^{1}H, br s, H-4) and 4.23 (^{1}H, br s, H-5)], a methyl group [δ_C 10.9 (q, C-7); δ_H 1.20 (3H, t, J 7.6 Hz, H-7)], a trisubstituted vinyl group [δ_C 180.1 (s) and 125.6 (d); δ_H 5.99 (^{1}H, s)], a methylene group [δ_C 23.0 (t); δ_H 2.42 and 2.63, (each ^{1}H, m)], as well as a keto carbonyl group [δ_C 202.8 (s)]. All these functionalities were assembled based on the COSY and HMBC spectra [22]. Specifically, in the HMBC spectrum the correlations of H-6 with C-2, C-3, and C-4 and of H-7 with C-3 suggested that C-2, C-4, and C-6 are connected to C-3. Other key correlations, H-2 to C-1 and C-5, revealed that C-1 is directly attached to C-2 and C-5 (Figure 7.8).

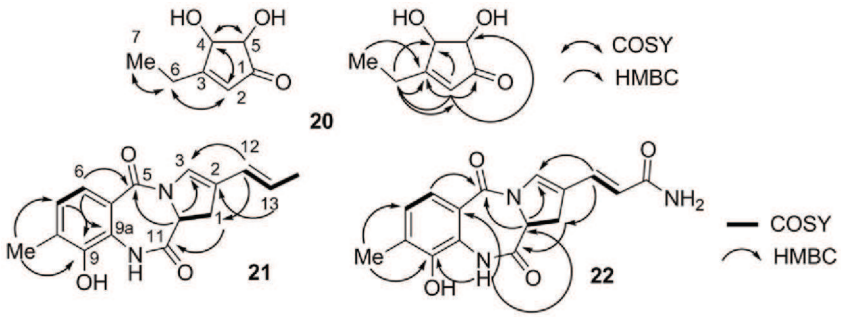

FIGURE 7.8 HMBC and COSY correlations of compounds **20–22**.

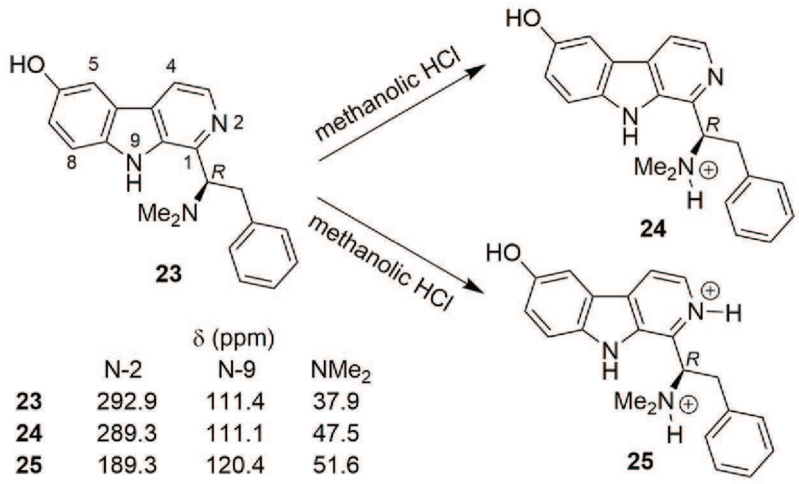

	δ (ppm)		
	N-2	N-9	NMe_2
23	292.9	111.4	37.9
24	289.3	111.1	47.5
25	189.3	120.4	51.6

SCHEME 7.2 Formation of dimethylammonium salt **24** and pyridiniumdimethylammonium disalt **25** of the marine alkaloid eudistomin X **23**.

In the case of the neuraminidase inhibitors limazepins G **21** and H **22**, the ^{1}H, ^{13}C NMR spectra together with DEPT experiments and a D_2O exchangeable assay for label protons indicate a pyrrolo[1,4]benzodiazepine skeleton. The combination of COSY, HMQC, and HMBC confirmed this proposal and led to the exact assignment of all ^{1}H and ^{13}C signals. In particular, the key HMBC correlations are: (1) H-6 with C-5 (amide carbonyl) and C-9a and H-7 with methyl and aromatic oxygenated carbons confirmed the substitution pattern of the benzene ring; (2) H-12 with C-1, C-3 and C-14 proves the anchorage of the 1-propenyl group at C-2 [23] (Figure 7.8).

All the referred and described HMBC spectra considered ^{1}H–^{13}C correlations but there are also other possibilities such as ^{1}H–^{15}N. This technique was used in the confirmation of the free-base **23**, dimethylammonium salt **24**, and pyridiniumdimethylammonium disalt **25** of the synthetic antimicrobial marine alkaloid eudistomin X. The ^{15}N NMR chemical shifts were indirectly acquired from the ^{1}H–^{15}N HMBC NMR experiments (Scheme 7.2). The ^{15}N resonance of the dimethylamino group presented only a minor deshielding in the mono salt **24** but the N-2 resonance shifted significantly upon protonation [24].

7.4 STEREOCHEMISTRY

The biological properties attributed to a wide range of chiral natural compounds are closely related to their stereochemistry and therefore, several approaches to determine the absolute configuration have emerged, based on NMR

spectroscopy. The establishment of the relative and absolute stereochemistry of stereogenic centers and the stereochemistry of geometric isomers is not an easy task. In some cases, it needs extensive NMR studies, chemical derivatizations together with NMR studies or total synthesis while the presence of isomers mixture led to an increased complexity in the ^{1}H and ^{13}C NMR spectra.

NOE (Nuclear Overhauser Effect) is a tool to establish a spatial relationship between atoms in a molecule. The NOE difference experiment detects and measures NOEs between protons through the space. It involves the application of a radio-frequency field to a single resonance in which the corresponding protons become saturated. Recording of the proton spectrum after the period of saturation may, therefore, show changes in signal intensities for the protons in the vicinity of the saturated proton. Thus, 1D NOE studies present the differences between the proton control spectrum and the irradiated proton spectra. In the 2D NOESY (Nuclear Overhauser Effect SpectroscopY) experiments, only one spectrum is recorded and contains all the information provided by the NOE studies.

A simple example for the utility of NOESY data is the establishment of the configuration of the C2′=C3′ double bond of geranylphenazinediol **6** (Figure 7.2). The correlation between 10′-Me and 1′-CH_2 as well as 2′-CH and 4′-CH_2 and the absence of correlation between 2′-CH and 10′-Me confirmed the (*E*)-configuration of this vinylic system [6]. In another example, the NOESY data was only useful for determining the (*E*)-configuration of the C8=C9 double bond of the tetraene chain of the antibacterial gombapyrone E **26**, since the remaining double bonds geometries were deduced by ^{1}H-^{1}H NMR coupling constants [25] (Figure 7.9).

The relative configuration of salimabromide **27**, a tetracyclic antibiotic compound possessing a brominated benzene ring, a furano lactone residue, and a cyclohexane ring, bridged by a seven-membered cyclic unit, was proved by the NOE connectivities and the (*Z*)-configuration of the C3=C9 double bond was assigned by NOE correlation between H-3 and H-9 and also supported by the ^{1}H-^{1}H NMR coupling constant ($J_{H\text{-}3,H\text{-}9}$ 13.1 Hz) [26] (Figure 7.9).

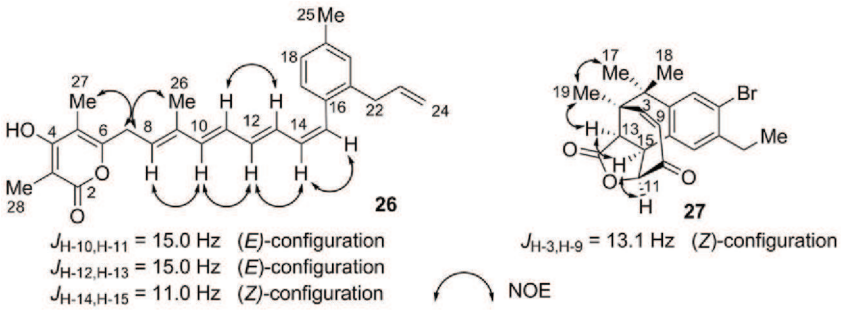

FIGURE 7.9 Stereochemistry of gombapyrone E **26** and salimabromide **27** established by NOEs.

The relative configuration of other marine natural products were elucidated by a combination of NOESY experiments and comparison with the ^{1}H and ^{13}C NMR data of known compounds [27], or using other techniques such as circular dichroism (CD) [28] and overall optical rotation [29].

Contrary to NOESY, ROESY (Rotating-frame Overhauser Effect SpectroscopY) is a quite useful technique for molecules with large molecular sizes (NOEs are too weak to be detectable). In NOESY the cross-relaxation rate constant goes from positive (for small molecules) to negative (for large molecules) as the correlation time increases, or even null, whereas in ROESY the cross-relaxation rate constant is positive for all rotational correlation times. This experiment, in which homonuclear NOE (ROE) effects are measured under spin-locked conditions, presents the signals that arise from proton resonances that are spatially close even if they are not bonded.

Five new potential cytotoxic austalides were isolated from the sponge-associated fungus *Aspergillus* sp. and their relative configuration was elucidated by interpretation of their ROESY spectra. For example, the correlations observed between 24-Me with H-21 and of 31-OMe with H-21 and 24-Me, indicates that rings C and D of austalide M **28** are *cis*-fused. The *trans*-configuration of 24-Me and 27-Me is due to the correlation between 27-Me and H-22 but not with H-21, establishing the (11*S**, 13*R**,14*R**, 20*R**, 21*S**, 22*S**)-relative configuration of **28** [30]. An extensive investigation on the same strain led to the isolation of seven new alkaloids. The correlations observed for both H-12 and 13-CH_2 with H-2, indicated a *cis*-orientation for H-2 H-12, and C-13, and assigns the (2*S**, 3*R**, 12*R**)-configuration of tryptoquivaline K **29** [31]. The relative stereochemistry of the two heterocyclic rings of the antibacterial and antitumor agent fradimycin A **30** was based on the ROESY correlations of H-1′ with H-5′, H-4′ with H-6′, H-7′′ with H-9′′, H-8′′ with H-10′′ and H-9′′ with H-13′′ [32]. The (*E*)-geometry of the two double bonds at C-12 and C-16 of the antibacterial and antitumor agent napyradiomycin A **31** was determined by the ROESY correlations between H-11 with H-12 and 13-CH3-Me and the absence of correlation between H-12 and 13-CH3-Me and also between H-19 with H-16, respectively [33]. ROESY data in combination with *J*-based configurational analysis was used to establish the relative configuration at C-11/C-12 and C-12/C-13 of 13-hydroxyprethyrsenol A **32**, an oxasqualenoid cytotoxic agent isolated from the red alga *Laurencia viridis* [34] (Figure 7.10).

The complexity in the ^{1}H spectrum can be enlarged by the presence of geometrical isomers in solution. Usually, the restricted rotation provided by the carbon–carbon double bond led to the appearance of two sets of signals corresponding to the rapid interconversion of the proton resonances of the *cis*- and *trans*-isomers or more generally, (*Z*)- and (*E*)-isomers. The ^{1}H NMR spectra of some antibacterial butenolides **33a,b** and **34a,b** (Figure 7.11), isolated from korean tunicate *Pseudodistoma antinboja*, showed these two spin signals with an integral ratio of 1:2, the (*Z*)-form being predominant. The difference in the structures of these two isomers is due to the configuration of C4 = C5, which can

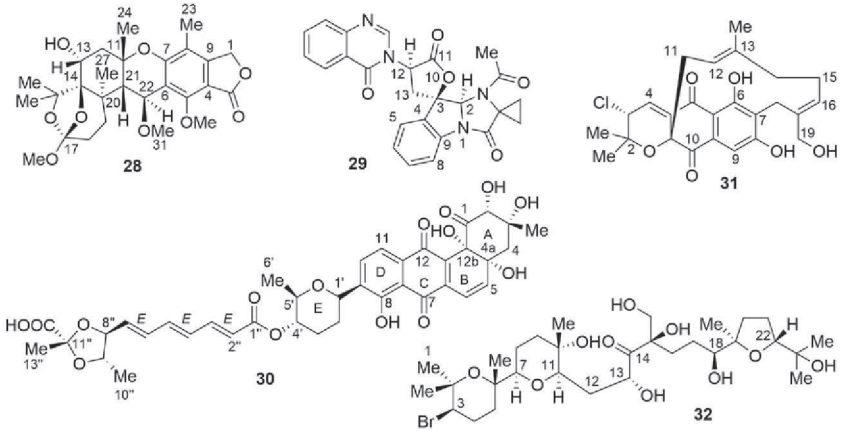

FIGURE 7.10 Structures of compounds **28–32**.

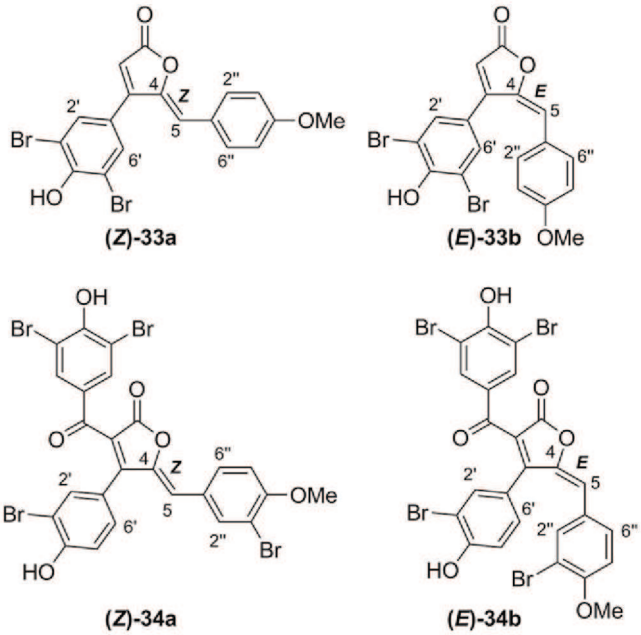

FIGURE 7.11 Geometric isomers of butenolides **33** and **34**.

be assigned by NOE difference experiments. Irradiation of H-5 of **33a** induced enhancements of H-2′,6′ and H-2′′,6′′ signals, indicating a (*Z*)-configuration for this vinylic system. In contrast, irradiation of H-5 of the (*E*)-isomer **33b**, induced NOEs of H-2′′,6′′. Moreover, irradiation of H-2′,6′ induced an

enhancement of H-2′′,6′′ indicating a close proximity between the two phenyl rings consistent with the (*E*)-configuration of C4=C5. In the case of isomers **34**, the ROESY spectra unequivocally identified the (*Z*)-isomer by the presence of two ROE cross-peaks of H-5 with H-2′,6′ and H-2′′,6′′. The location of the methoxyl group at C-4′′ was assigned by the ROESY correlations between the methoxyl protons and H-5′′ [35].

As shown earlier, NOE and ROE experiments are very useful in establishing the stereochemistry of vinylic and chiral compounds. However even with these techniques is still very difficult to assign the stereochemistry of highly flexible chains due to the presence of multiple conformers. In these cases, minor populations often originate large NOEs, occasionally leading to contradictory conclusions. Trying to solve this problem, Murata and his group developed a method for the relative configuration analysis of natural products based on ^{13}C-^{1}H spin-coupling constants ($^{2}J_{C,H}$ and $^{3}J_{C,H}$) and ^{1}H-^{1}H spin-coupling constants ($^{3}J_{H,H}$) [36,37]. They conclude that the relative stereochemistry assignment of acyclic systems, where the conformation of adjacent asymmetric centers is represented by staggered rotamers, can only be determined by the combination of these coupling constants, since they allowed the identification of the predominant staggered rotamer out of the six possible from the *threo* and *erythro* configurations, while using $^{3}J_{H,H}$ is inadequate because two H/H-*gauche* rotamers cannot be distinguished. $^{3}J_{C,H}$ follow a Karplus-type equation (Figure 7.12c) and can be used for stereochemistry analysis as is the case of $^{3}J_{H,H}$ (Figure 7.12a). Therefore, when an oxygen functionality on a carbon atom is *gauche* to its geminal proton $^{2}J_{C,H}$ becomes large, and when it is *anti*, the value becomes small (Figure 7.12b).

To assign the stereochemical relationship of a pair of vicinal asymmetric carbons (1,2-methine systems) commonly found in natural products, we have to choose a single conformer with a correct configuration of staggered rotamers possible in *threo*- and *erythro*-diastereomers (Figure 7.13). Four conformers A-1, A-2, B-1, and B-2 can be identified based on $^{3}J_{H,H}$, $^{2}J_{C,H}$, and $^{3}J_{C,H}$ but the other two A-3 and B-3 bearing a H–H *anti*-orientation cannot be distinguished.

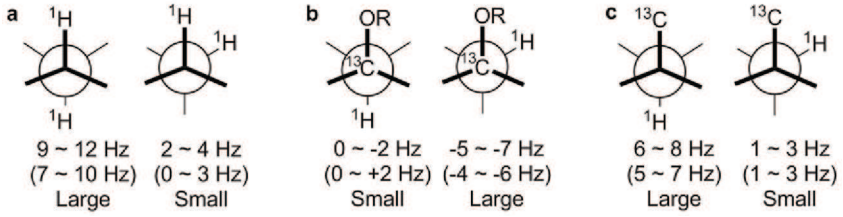

FIGURE 7.12 Dihedral angle dependence of spin-coupling constants: (a) $^{3}J_{H,H}$ for *anti*- and *gauche*-rotamers; (b) $^{2}J_{C,H}$ when dihedral angles between ^{13}C-attached oxygen and the proton are 180° and 60°; (c) $^{3}J_{C,H}$ when the dihedral angles are 180° and 60°. The figures in parentheses represent the values of 1,2-dioxygenated systems. *Adapted from [36].*

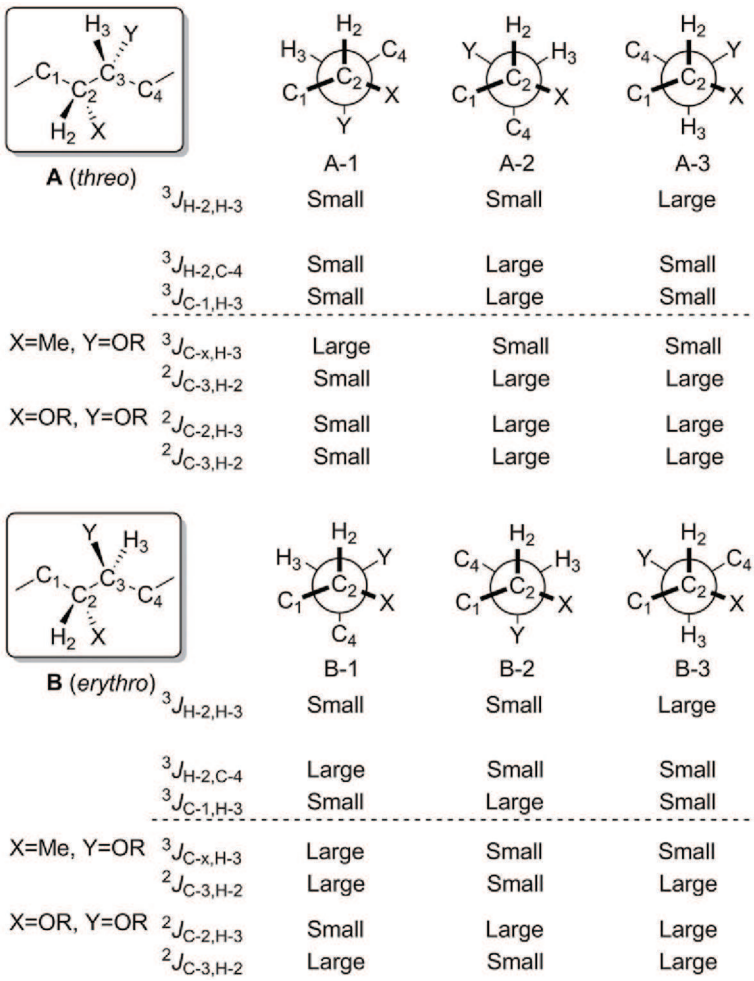

FIGURE 7.13 Dependence of $^3J_{H,H}$ and $^{2,3}J_{C,H}$ on dihedral angles between vicinal 1,2-methine carbons in butane systems. Occurring pairs of substituents in natural products, Me/OR and OR/OR, are presented. (Me/Me is omitted since it rarely occurs in natural products.) R stands for H, alkyl, and/or acyl groups. *Adapted from [35].*

For these *anti*-conformers, NOE experiments are a practical way to assign their configurations although they are structure dependent [36].

Murata and his group described similar strategies for 1,3- and 1,4-methine systems [36]. This type of comprehensive configuration analysis of complicated natural products based on $^{13}C–^1H$ coupling constants are scarce in the literature, probably due to the difficulty in determining the $^{2,3}J_{C,H}$ values accurately.

Sato *et al*. used the Murata's method to establish the relative configuration of three substructures (C-4 to C-13, C-31 to C-34, and C-20 to C-42) of the neomaclafungin A **5**, the most abundant compound of the new neomaclafungins

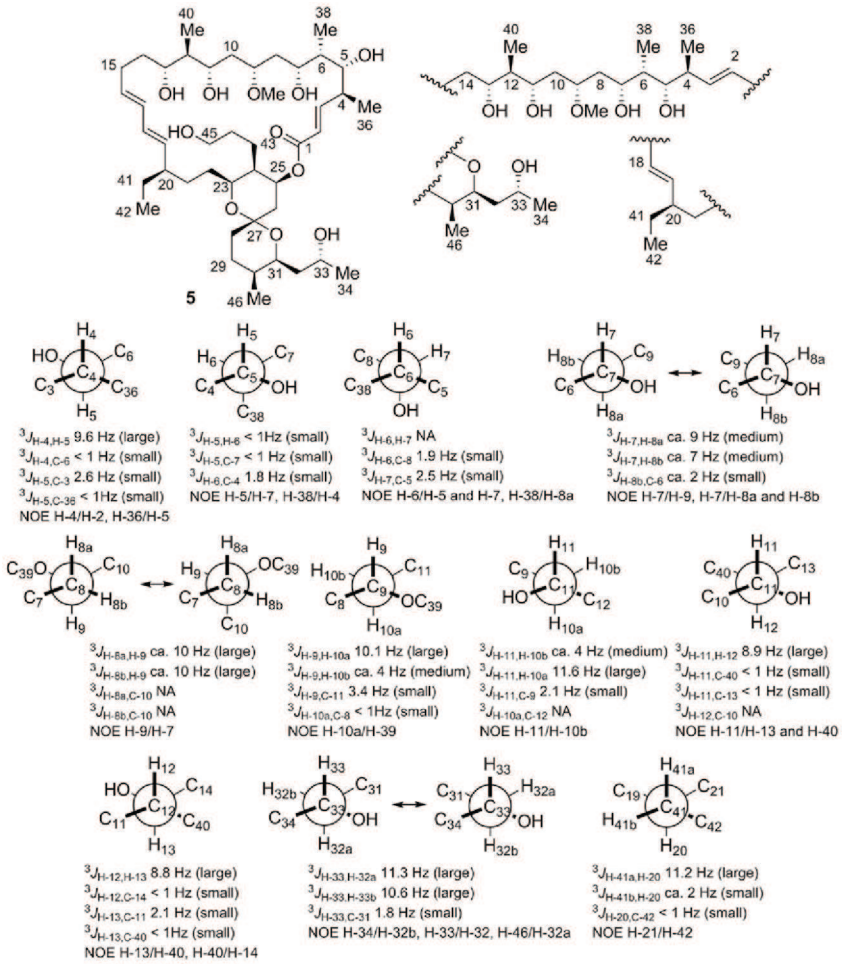

FIGURE 7.14 Stereochemistry establishment of the stereogenic centers of neomaclafungin A **5**. *Adapted from [5].*

A-I macrolides isolated from a marine actinomycete (Figure 7.14). The configuration of C-4 to C-6 was based on the H-4 and H-5 assignments. Their *anti*-orientation was assigned by the large $^3J_{H\text{-}4,H\text{-}5}$, small $^3J_{H\text{-}5,C\text{-}3}$, and small $^3J_{H\text{-}4,C\text{-}6}$ values. The orientation of H-4 *gauche* to 5-OH and *anti* to H-5 was supported by the NOE correlation of H-36 with H-5. The coupling constant values of $^3J_{H\text{-}7,H\text{-}8a} \sim 9$ Hz, $^3J_{H\text{-}7,H\text{-}8b} \sim 7$ Hz, and $^3J_{H\text{-}8b,C\text{-}6} \sim 2$ Hz led the authors to consider two major rotamers around the C-7 and C-8 carbon bond where H-5 and the two H-8 exhibit both *gauche*- and *anti*-orientations. All the other relative configurations were elucidated by the same method (Figure 7.14) [5].

Another approach for the assignment of relative and absolute configuration of acyclic compounds is based in the Universal NMR Database developed by

Kishi's group [38,39]. It is an empirical procedure that relies on the comparison of the observed chemical shifts of compounds with unknown vicinal or proximal centers with libraries of configurationally known stereomodels. These ^{1}H and ^{13}C NMR databases were first created for the stereochemical assignment of 1,3,5-triols [37,38,40] and then extended for 1,2,3-triols, 1,2,3,4-tetraols, and 1,2,3,4,5-pentaols [41–43]. Using this strategy, the relative configuration of 1,3-diol system at C7/C-9 of caylobolide B **12** was assigned as a *syn*-arrangement since it fits with the carbon chemical shifts of a 1,3-diol model system. The 1,3,5-triol unit was assigned as either *syn*/*anti* or *anti*/*syn* between C-25/C-27 and C-27/C-29, comparing the carbon chemical shifts at C-27 with those of the central carbon of the 1,3,5-triol model system (Figure 7.15). This method cannot differentiate between *syn*/*anti* or *anti*/*syn* orientation. Mosher's method (see later) was also inconclusive on the absolute configuration of **12**, due to the small amount of the sample [12].

The stereochemistry of chiral marine natural products can also be determined based on chiral derivatizing agents (CDA) and ^{1}H NMR experiments. This methodology requires the transformation of a chiral substrate into two different species, by derivatization of one enantiomeric substrate with chiral auxiliary reagents to give two diastereomers or conformers, which can be differentiated by NMR. This can be achieved by two main approaches in which a pure enantiomeric substrate is separately derivatized with two enantiomers of the chiral auxiliary (double derivatization) or with a single enantiomer of the chiral auxiliary (single derivatization). In the former case, the chiral substrate is derivatized with the two enantiomers of the chiral auxiliary (*R* and *S*) and the ^{1}H NMR spectra of the obtained diastereomers are compared between them. In the latter case, the chiral substrate is coupled with only one enantiomer of the chiral auxiliary (either *R* or *S*), and the ^{1}H NMR of the resulting diastereomer is recorded. Then, a conformational change is induced (e.g., temperature change or chelate formation) and a second ^{1}H NMR spectra is taken. The differences between these two spectra and their comparison with the induced conformational changes correlate the configuration of the substrate with that of the reagent. Another option does

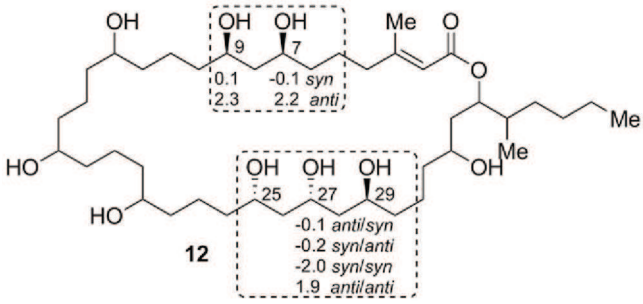

FIGURE 7.15 Difference in the ^{13}C NMR chemical shifts of 1,3-diol and 1,3,5-triol of caylobolide B **12** with those of similar model systems.

not involve conformational changes, but a simple comparison of the diastereomer spectrum with that of the substrate prior to derivatization.

As described earlier, two different spectra are always obtained and compared. The sign of the differences in the chemical shifts of the substituents of the asymmetric carbon of the substrate in the two diastereomers (or conformational species) provides information about the configuration of this asymmetric center. For example, in the Mosher's method a chiral secondary alcohol can be derivatized with (*R*)- and (*S*)-α-methoxy-α-phenylacetic acid (MPA) or with α-methoxy-α-trifluoromethyl-α-phenylacetic acid (MTPA) and the differences in the chemical shifts $\Delta\delta^{RS}$ for MPA and $\Delta\delta^{SR}$ for MTPA calculated. $\Delta\delta^{RS}$ is the difference between the chemical shift in the (*R*)-MPA ester derivative and that of the (*S*)-MPA while $\Delta\delta^{SR}$ is the difference between the chemical shift in the (*S*)-MTPA ester derivative and that of the (*R*)-MTPA [44,45].

Since the original Mosher's method [46,47], NMR procedures for the assignment of absolute configuration of chiral compounds have been improved and a large number of CDAs is available for the study of different substrates. The most common one is α-methoxy-α-trifluoromethyl-α-phenylacetic acid (MTPA) known as Mosher's reagent, α-methoxy-α-phenylacetic acid (MPA), α-methoxy-α-(2-naphthyl)acetic acid (2-NMA), α-(9-anthryl)-α-methoxyacetic acid (9-AMA), Boc-phenylglycine (BPG), among others. Over the years, the scope of Mosher's method has been expanded to highly hindered secondary (*sec*) alcohols, primary (*prim*) alcohols, tertiary alcohols, primary and secondary amines, and of *sec*/*sec*, *sec*/*prim*, or *prim*/*sec* 1,n-diols and 1,2-amino alcohols, and carboxylic acids [44,45,48].

Mosher's method can use ^{19}F NMR, particularly the chemical shifts of the CF_3 groups, and ^{1}H and ^{13}C NMR, namely the chemical shifts of the protons and carbons of the chiral alcohol under study, to deduce the absolute configuration of the substrate based on the signs of the Δδ values and using certain empirical models [44]. In this chapter the ^{1}H NMR models will be described since it is the most frequently used in the literature. This model is based on the anisotropic effect that the α-phenyl group of the auxiliary MPA and MTPA exerts on the substituents Z^1 and Z^2 of the alcohol. This effect establishes a correlation of the spatial position of Z^1 and Z^2 with respect to the phenyl of the MPA and MTPA moieties, based on the signs of, respectively, $\Delta\delta^{RS}$ or $\Delta\delta^{SR}$ of the substituents. In these methods it is assumed that the most representative conformation have H-1′, the carbonyl group and the methoxyl group in the same plane in the case of MPA and H-1′, the carbonyl group and the trifluoromethyl group in the same plane in the case of MTPA [44] (Figures 7.16 and 7.17).

The protons of the substituent Z^2 are shielded in the (*R*)-MTPA ester while those of the Z^1 remain unaffected. In the (*S*)-MTPA ester the opposite occurs: Z^1 are shielded while those of the Z^2 remain unaffected. These shieldings are expressed as $\Delta\delta^{SR}(Z^1) = \delta Z^1(S) - \delta Z^1(R)$ and $\Delta\delta^{SR}(Z^2) = \delta Z^2(S) - \delta Z^2(R)$. All the protons shielded in the (*R*)-MTPA derivative will present a positive $\Delta\delta^{SR}$ while those shielded in the (*S*)-MTPA ester will present a negative $\Delta\delta^{SR}$ value (Figure 7.16).

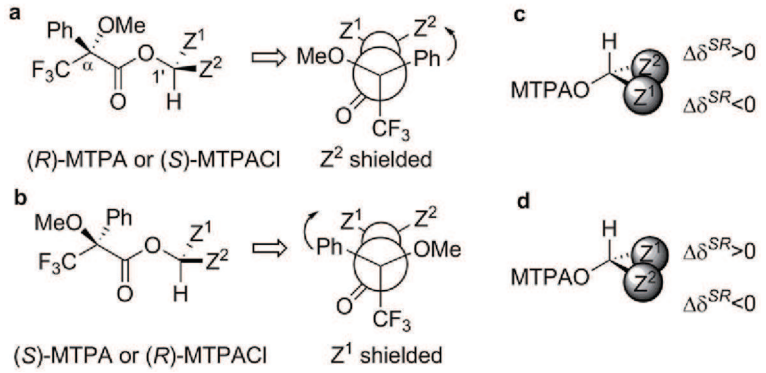

FIGURE 7.16 Model for configurational correlation of MTPA esters: (a, b) assignment by ^{1}H NMR and (c, d) expected sign of $\Delta\delta^{SR}$. *Adapted from [44].*

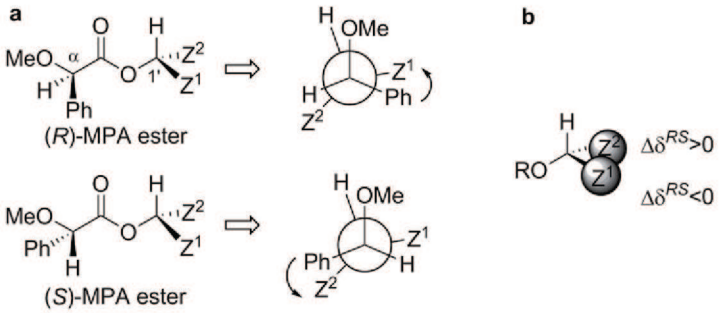

FIGURE 7.17 Model for configurational correlation of MPA esters: (a) assignment by ^{1}H NMR and (b) expected sign of $\Delta\delta^{RS}$. *Adapted from [44].*

In the case of the (*R*)-MPA ester substituent Z^1 is shielded by the phenyl ring whereas Z^2 is unaffected. In the case of the (*S*)-MPA ester substituent Z^2 is shielded whereas Z^1 is unaffected (Figure 7.17) [44].

The absolute configuration of two new and two already known potential antifungal and antitumoral azaphilones, isolated from the endophytic fungus *Chaetomium globosum*, were determined by the Mosher's method [49]. A solution of the new 5′-epichaetoviridin A **35** (Figure 7.18) in dichloromethane was treated with (*R*)- or (*S*)-MPA acids and the mixture was stirred at room temperature for 24 h. The two diastereomeric esters were purified by column chromatography and the analysis of their ^{1}H NMR spectra revealed positive $\Delta\delta^{RS}$ values for H-4′ and 4′-Me (+0.101 and +0.105, respectively) and a negative value for H-6′ (−0.175), that applying the MPA criteria, assigns (*S*)-configuration for C-5′ in compound **35**. A similar procedure was used for the preparation of the (*R*)- and (*S*)-MTPA esters of the known chaetoviridin D **36** (Figure 7.18). Their ^{1}H NMR data revealed negative $\Delta\delta^{SR}$ values for H-10, H-11 and 11-Me

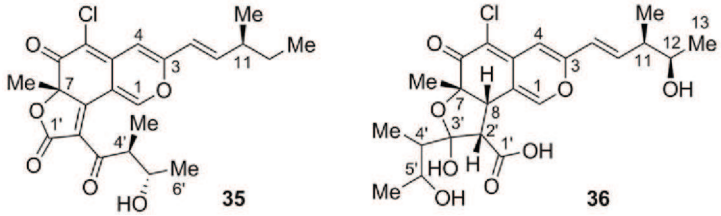

FIGURE 7.18 Structures of 5′-epichaetoviridin A **35** and chaetoviridin D **36**.

(−0.14, −0.062, and −0.086, respectively) and a positive $\Delta\delta^{SR}$ value for H-13 (+0.043) that following the MPTA rules, assigns the (*R*)-configuration of the secondary hydroxyl group at C-12. It was not possible to determine the C-5′ configuration by this method because it was not possible to derivatize the secondary alcohol linked to this carbon. Comparative analysis of the ^{1}H NMR data of chaetoviridin D **36** with chaetoviridin A already reported [50] suggested (*S*)-configuration at both C-7 and C-11. NOE experiments also confirmed this disposition.

Advanced Mosher's method was also quite useful in elucidating the absolute configuration of the fijiolides A **37** and B **38**, inhibitors of TNF-α-NF-kB activation obtained from a marine-derived bacterium of the genus *Nocardiopsis*, that possess in their structures an aminosugar, an NH group, and an OH group [51].

The absolute configuration of the ribopyranose moiety was determined by the calculation of $\Delta\delta^{SR}$ values of the bis-MPTA esters of fijiolide A **37a,b** (Figure 7.19) that indicate (*R*)-configuration at C-2′, allowing the establishment of the stereochemistry of the remaining chiral centers of the ribopyranose moiety as (1′*S*, 2′*R*, 3′*R*, 4′*S*) based on the vicinal coupling constants ($^{1}J_{\text{C-1',H-1'}}$, 161 Hz indicates a β-configuration for the anomeric carbon, $^{3}J_{\text{H-1',H-2'}}$, 8 Hz indicates an axial configuration for H-2′) and NOESY spectroscopy data (NOE of H-2′ with H-3′ and of H-3′ with H-4′ establish that H-2′ and H-3′ are in the axial and equatorial positions, respectively).

The absolute configuration at C-17 was elucidated by the ^{1}H NMR data of MTPA amides of fijiolide B **38a,b** (Figure 7.19) that presented positive $\Delta\delta^{SR}$ values for H-19 and H-23 and negative $\Delta\delta^{SR}$ values for H-16, assigning the (*S*)-configuration at this carbon. To assign the absolute configuration at C-13, the 1,2-diol groups first were protected and then the MTPA derivatization was performed. Calculation of $\Delta\delta^{SR}$ values of the MPTA esters of fijiolide A **37** indicates an (*R*)-configuration at C-13. The absolute configuration of the remaining C-8 and C-9 were established by the correlations presented in the NOESY spectra [51].

The absolute configuration of eunicidiol **39**, a potent anti-inflammatory agent, was unambiguously assigned by the Mosher's method. Comparing the ^{1}H NMR data of the (*S*)-MPA ester **41** of the eunicidiol **39** with that of the corresponding (*R*)-MPA ester **40**, H-10, H-17, and H-18 of the former were strongly shielded by the phenyl ring while H-16a,b were less shielded. Thus, the $\Delta\delta^{RS}$

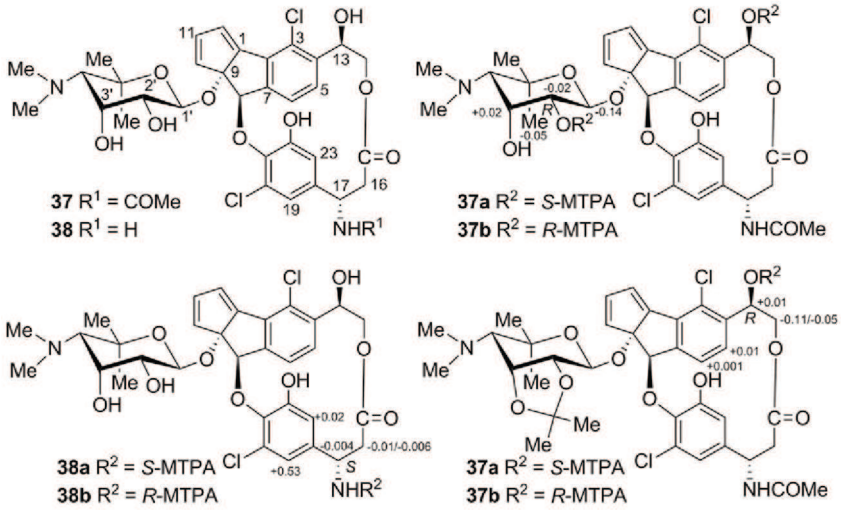

FIGURE 7.19 Chiral derivatization products of fijiolide A **37** and B **38**.

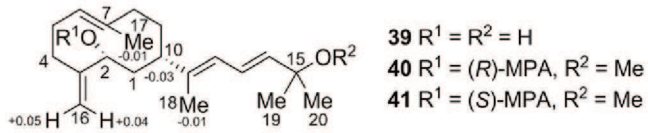

FIGURE 7.20 Structures of eunicidiol **39** and corresponding (*R*)- and (*S*)-MPA esters **40** and **41** and the $\Delta\delta^{RS}$ data for the MPA esters **40** and **41**.

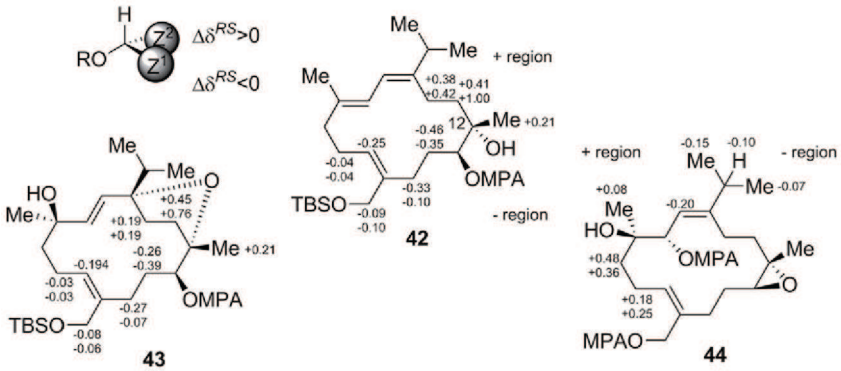

FIGURE 7.21 The $\Delta\delta^{RS}$ data for the MPA esters of sinulariols A **42**, D **43**, and L **44**.

values indicate the (2*R*)-configuration, which combined with the NOESY NMR data, provided the absolute configuration of **39** as (2*R*,10*S*) [52] (Figure 7.20). A similar procedure was applied to determine the absolute configuration of C-12 of the antimicrobial sinulariols A **42**, D **43**, and L **44** [53] (Figure 7.21).

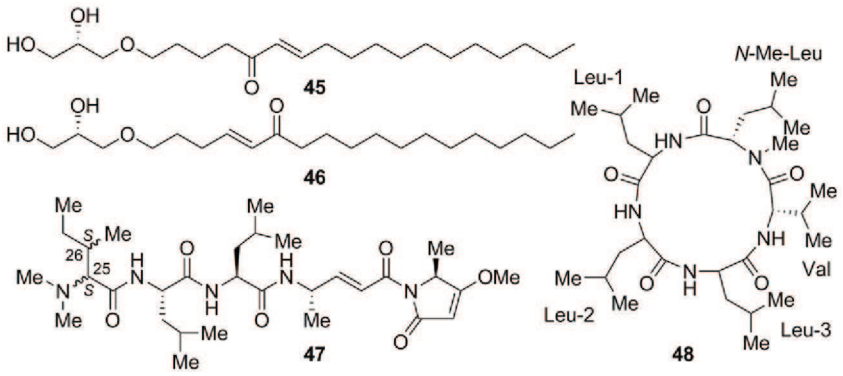

FIGURE 7.22 Structures of compounds **45–48**.

The total synthesis of marine natural products and the comparison of the spectra from the synthetic samples with those of the natural ones assigns the stereochemistry of the natural compounds. For example, the structures of the androgen receptor antagonists niphatenones A **45** and B **46** were assigned by NMR and MS data and confirmed by total synthesis [54]. A comparison of the NMR data of the isolated antimalarial agent gallinamide A **47** and of the four synthetic diastereomers assigned the absolute configuration as (25*S*,26*S*) at the *N*,*N*-dimethylated isoleucyl residue (Figure 7.22). Besides that, it helped to demonstrate that no tautomerization and epimerization reactions took place in the preparation of the analogues and the retention of the stereochemical integrity in the key steps [55].

The planar structure of the antimicrobial lajollamide A **48** (Figure 7.22), a cyclopentapeptide isolated from marine fungus *Asteromyces cruciatus*, was determined by NMR spectroscopy in combination with mass spectrometry but the absolute configuration was unambiguously solved by total synthesis [56]. This synthetic sequence provided three additional unnatural diastereomers and showed that the unexpected acid-mediated epimerization of leucine units in the lajollamide framework can be a danger in misassigning natural products structure when elucidated by spectroscopic methods alone.

In the case of the thrombin and Factor VIIa inhibitor dysinosin A **49**, the structure was determined by detailed NMR studies and its absolute stereochemistry deduced from an X-ray structure of a complex with thrombin [57]. Therefore, the total enantioselective synthesis of dysinosin A **49** provides definitive evidence for its structural and configurational identity [58] (Figure 7.23).

The structure of elisabethin A **50**, which was also named elisabethane, was established by spectroscopic methods and confirmed by an X-ray diffraction experiment, which also yielded its relative stereochemistry [59]. However, the absolute configuration of this molecule was not determined by the X-ray experiment, being accomplished only by their total synthesis [60]. The same occurred

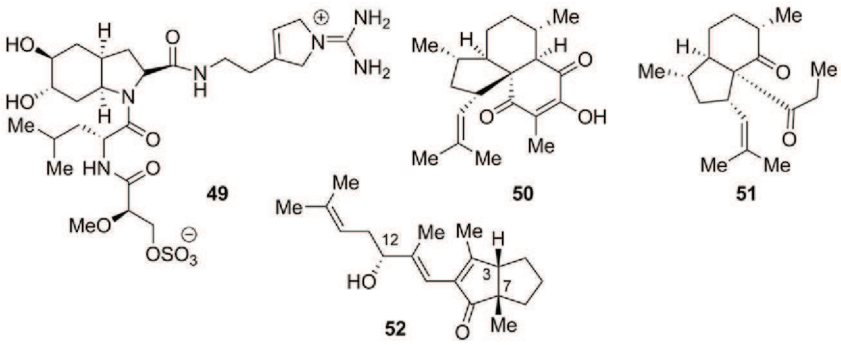

FIGURE 7.23 Structures of compounds **49–52**.

with elisabethin C **51**, a *bisnor*-elisabethane skeleton possessing antituberculosis activity [61] (Figure 7.23).

The structure of xestenone **52**, a marine norditerpenoid found in the northeastern Pacific sponge *Xestospongia vanilla*, was established by spectroscopic methods and the relative configuration of their C-3 and C-7 stereogenic centers determined by NOESY spectral analysis. However, the relative configuration of C-12 and the absolute configuration of this compound were only successfully determined by their total synthesis [62] (Figure 7.23).

7.5 HYPHENATED NMR TECHNIQUES

In the last decades, a large variety of publications have emerged involving NMR spectroscopy hyphenated to other techniques to provide useful information for the structural elucidation on the metabolites prior to isolation.

HPLC-NMR (High Pressure Liquid Chromatography coupled to Nuclear Magnetic Resonance) spectroscopy has been successfully used in the identification of metabolites of crude extracts of marine natural products. An advantage of this technique includes recovery of all components *in situ* for further analytical or biological assays and is a nondestructive experiment. The LC-NMR experiments can be performed by on-flow and stop-flow approaches. In the on-flow mode of operation, each fraction of the crude extract is subjected to the LC analysis and subsequent online ^{1}H NMR analysis, a valuable insight for the identification of major components. The limited sensitivity of this approach was increased by the introduction of the stop-flow mode. In the stop-flow measurements, selected chromatographic peaks are trapped in the LC-NMR flow cell and retained for the required period to extend the NMR acquisition times, allowing sensitivity and resolution of the 1D and 2D NMR spectra obtained.

The first reports using this hyphenated technique for the structure elucidation of marine natural products was conducted by Bobzin *et al.* in 2000, taking

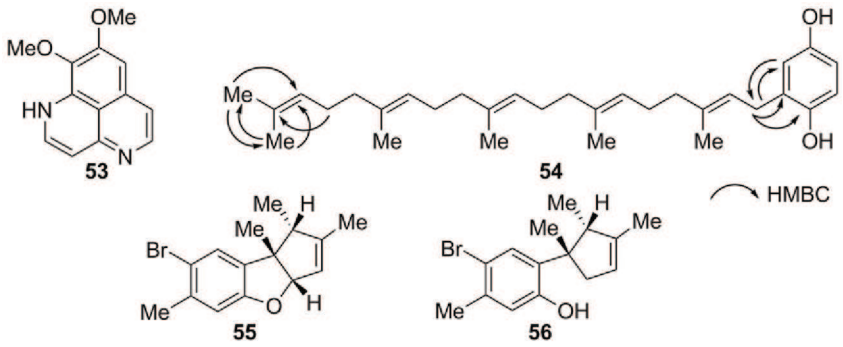

FIGURE 7.24 Structures of compounds **53–56**.

advantage of the new probe designs that allowed the use of gradient pulse sequences to provide efficient and specific suppression of the NMR signals due to the HPLC solvents. LC-NMR has been applied to identify the marine alkaloid aaptamine **53** as the active component (glutamine:fructose-6-phosphate amidotransferase inhibitor) in the crude dichloromethane extract of the sponge *Aaptos* sp. [63,64] (Figure 7.24). Since then, other bioactive compounds have been isolated and characterized (^{1}H, ^{13}C, COSY, ROESY, and one-bond and long-range heteronuclear correlations) from fungal isolates derived from marine sponges using this online stop-flow approach [65,66].

Later, Urban and her group dedicated their more recent works in the identification of several Australian marine natural products using on-flow and stop-flow protocols with a WET solvent suppression sequence [67]. They identified the antitumoral pentaprenylated *p*-quinol **54** as the major constituent in the dichloromethane extract of the marine sponge *Dactylospongia* sp. involving 1D (^{1}H, ^{13}C, and DEPT spectra) and 2D (COSY, HSQC, and HMBC spectra) NMR experiments [68]. Similar studies on the marine alga *Laurencia filiformis* led to the identification of the new potential antimicrobial compounds cycloisoallolaurinterol **55** and isoallolaurinterol **56** from their crude extract as well as the *in situ* monitoring of the chemical conversion between them [69] (Figure 7.24).

Using these strategies, in the crude extract of *Laurencia elata* it was possible to identify, by 1D (^{1}H, ^{13}C, DEPT, and NOE experiments) and 2D (COSY, HSQC, and HMBC spectra), NMR techniques, two novel potential antitumoral C_{16} chamigrenes, cycloelatanene A **57** and B **58**, and several previously reported compounds [70]. In the red alga *Plocamium angustum*, the identification of the cytotoxic agent plocamenone **59** and the unstable double bound isomer isoplocamenone **60** was achieved (Figure 7.25). Conventional offline chemical investigations allowed the structural revision of the former compound as well as the collection of sufficient amount for the biological assays [71]. More recently, seven resorcinol and two polyene secondary

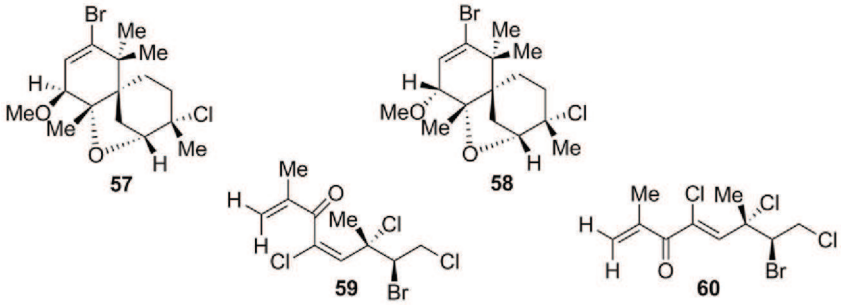

FIGURE 7.25 Structures of compounds **57–60**.

metabolites were obtained from the crude dichloromethane extract of the marine brown alga *Cystophora tondosa* [72]. In most cases, for completion of the structural elucidation, the compounds were isolated by preparative HPLC and subjected to NMR and MS (Mass Spectrometry) measurements. Although the online LC-NMR-MS technique gained an increased importance for a rapid isolation and identification of complex mixtures in clinical, biological, and natural products research [73], to the best of our knowledge the benefits of this hyphenated protocol has not been applied in the field of marine natural products investigation.

SPE (Solid Phase Extraction) coupled to the LC-NMR system emerged in recent years in order to increase the amount of analyte in the flow cell. As the SPE cartridge is placed after the HPLC separation, this approach presents several advantages that reduces drastically the analysis costs: (1) increased amount of sample; (2) HPLC separation without deuterated solvents; (3) wide range of solvents and gradients in the HPLC separation. After the collection of the analyte in the cooled nitrogen SPE cartridge, it is dried with a stream of nitrogen and finally washed with a deuterated solvent prior to injection in the NMR flow cell. A final advantage of this LC-SPE-NMR technique is the use of low-volume probes to maximize sample concentration and NMR data quality [67]. In this field, several reports have appeared, providing comprehensive information about novel products obtained directly from plant crude or prepurified extracts [67,74]. However, the application of this methodology to marine natural products is quite scarce. A single example uses a HPLC-SPE-NMR setup coupled to a diode array detector (DAD) monitoring HPLC separation and triggering SPE trappings. A HPLC-DAD-SPE-NMR system was used to resolve complex natural isolates of marine-derived *Streptomyces* spp. in which four known and 12 new rare reveromycin classes (Figure 7.26 shows two examples of these compounds **61** and **62** and the corresponding key NMR correlations) of antiproliferative polyketide spiroketals were identified. These results were supported by further mass spectrometry analysis using a separate HPLC-DAD-MS installation [75].

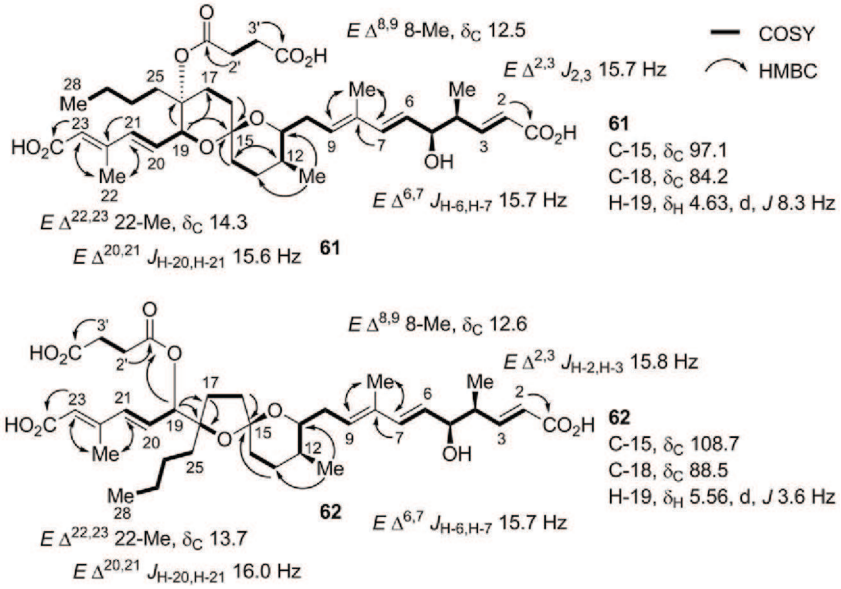

FIGURE 7.26 Key 2D NMR correlations of the 6,6-spiroketal **61** and 5,6-spiroketal **62**.

7.6 QUANTITATIVE NMR

High-resolution NMR spectroscopy is an almost unique tool in the quantitative evaluation of mixtures: it is nondestructive and with a few precautions in terms of parameter choice [76] the integral intensity of a given signal is directly proportional to the number of nuclei contributing to that signal; that is, intensities directly reflect molar ratios. Unlike optical spectroscopy, no calibration is required, and it is not necessary to make assumptions about the identity of the compounds to be determined. Further, compared to quantification based on chromatographic separation, there is no risk (except for enantiomers, since they present the same NMR spectrum) of not being able to resolve the different components. However, a number of factors can distort signal intensities [77].

1D and 2D proton quantitative NMR (qHNMR) has proved to be highly suitable for the simultaneous selective recognition and quantitative determination of metabolites in complex biological matrixes, such as quantitation of single natural products in plant extracts, dietary materials, and materials representing different metabolic stages of (micro)organisms. As a general rule, qHNMR provides an opportunity for the routine determination of constituents at the 1% level with 1% error and is well capable of analyzing possibly down to the 0.1% level and below with errors as low as 0.1%, depending on the nature of the sample [78].

Quantitative NMR possesses the required accuracy and precision to become a routine quantitative tool in many analytical laboratories. Chemical referencing

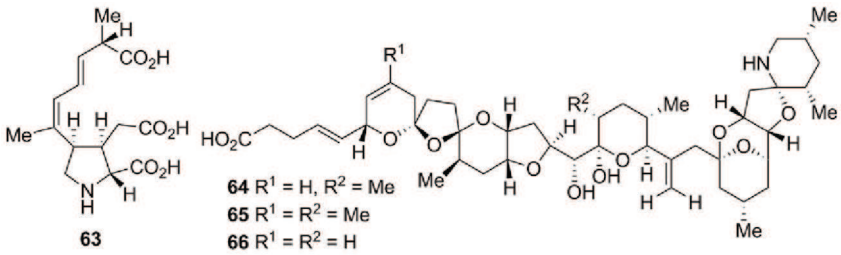

FIGURE 7.27 Structures of compounds **63–66**.

with internal standards can provide accurate quantification, but this technique contaminates the sample. As a consequence the use of external references or the use of ^{13}C satellites as an internal standard in 1H NMR spectroscopy allows this contamination problem to be circumvented. It is noteworthy to notice the ability of this method to function accurately with external calibration, requiring only nonidentical calibrants, and simultaneously quantitating several compounds [79].

Although both internal and external referencing methods have been used, several electronic referencing approaches have also been reported in an attempt to provide accurate and precise quantitative results. A very recent publication makes a comparison of quantitative nuclear magnetic resonance methods using internal, external, and electronic referencing [80].

Burton *et al*. [81,82] discussed the application of qHNMR with external standards (e.g., caffeine) for monitoring phycotoxins (e.g., domoic acid **63**; Figure 7.27), a challenging task because their isolation from marine matrixes such as shellfish or plankton is tedious and generally presents a total yield of low milligram to submilligram range. They concluded that qHNMR has the potential for accurate determination of molar phycotoxin concentrations in crude extracts of marine organisms. This method was used to accurately certify the concentration of certified calibration solutions of the potent marine biotoxins azaspiracid-1 **64**, -2 **65,** and -3 **66** [83] (Figure 7.27).

qHNMR was used to quantify pyrrole-2-carbaldehyde derivatives in the extracts of wild and cultured sponges, using 4-hydroxy-3-methoxybenzaldehyde (vanillin) as an internal standard [84] and also to determine the concentration of stevensine **67** (Figure 7.28) in butanol partitions of crude extracts from the sponge *Axinella corrugate*, using cyclooctatetraene as an internal standard [85]. Compound **67** showed deterred feeding in laboratory aquarium assays.

The Molinski group developed a simple and accurate method for quantitation of small amounts of natural products, taking advantages of the developed technologies in microcoil probes and narrow diameter tube microprobes [86]. They used the solvent ^{13}C-satellites (QSCS) method for the quantitation, which uses the integration of ^{13}C satellite peaks of deuterated solvents, in particular

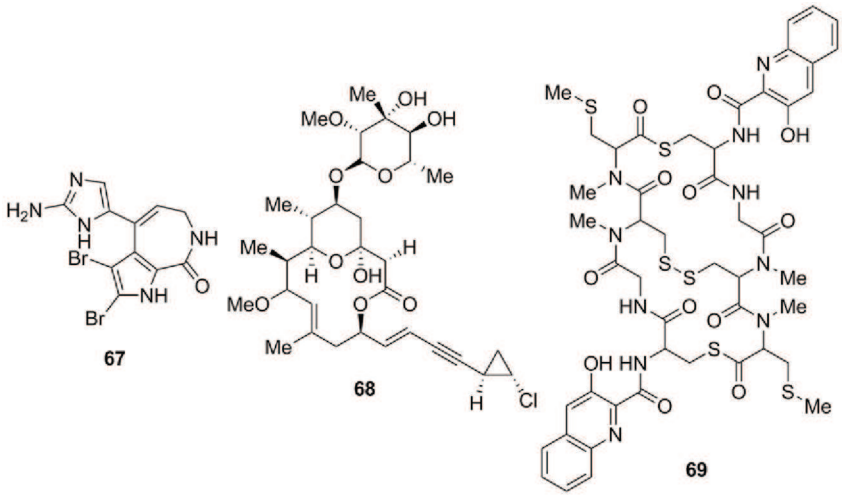

FIGURE 7.28 Structures of compounds **67–69**.

$CDCl_3$, that have favorable intensities for measurements of samples in NMR microcoils and microprobe tubes in the 1 to 200 nanomole range. Highly sensitive cryoprobes allow ready observation of the so-called ^{13}C-satellites of the $^{13}CHCl_3$ signal ($^{1}J_{C\text{-}H}$ 209 Hz), even after only one scan. Although the main $^{12}CHCl_3$ signal intensity is generally too large for accurate quantitation of nanomole samples due to dynamic range considerations, the $^{13}CHCl_3$ solvent satellite integrals are comparable in magnitude to those of typical methine CH signals in the natural product sample being measured. They concluded that the number of moles of a sample, *m*, in a $CHCl_3$ solution is related to the ratio of a signal integral A_{CH} to satellite integrals A_{sat} by a proportionality constant, *c*. This constant may be obtained from the slope of a standard curve of the ^{1}H NMR integral ratio for methine signals of a standard sample, A_{CH}, to residual $^{13}CHCl_3$ integral, A_{sat}, against the amount of a standard in a fixed volume of sample $CDCl_3$ solution.

$$\begin{aligned} m &= (A_{CH} / A_{sat}) / c \\ A_{sat} &= A_L + A_R \ (A_L \text{ being the left-hand and } A_R \text{ right-hand} \\ &\quad \text{components of the } {}^{1}H\text{-}{}^{13}C \text{ couplet of residual } {}^{13}CHCl_3) \\ A_{CH} &= \text{integral of a methine signal} \end{aligned} \tag{7.1}$$

After establishing the proportionality constant, *c*, in a specific spectrometer, we can apply Eq. (7.1) to determine the amount of a specific metabolite in a $^{13}CHCl_3$ solution. The method was illustrated for the structure elucidation and the quantitation of a new potential cytotoxic natural product phorbaside F **68** from the marine sponge *Phorbas* sp. (Figure 7.28).

QSCS expands the window of discovery and characterization of new natural products, especially those that can be procured only in vanishingly small amounts [87,88].

qHNMR is very useful tool for determining metabolite concentration, but sometimes severe signal overlapping of complex metabolite mixtures hinders the accurate quantification. Markley *et al*. [89] have developed a 2D extrapolated time-zero ^{1}H-^{13}C HSQC ($HSQC_0$) to simultaneously quantify and identify individual chemicals in metabolite mixtures. In this method, the extension of 1D ^{1}H to 2D ^{1}H-^{13}C HSQC leads to the dispersion of peaks along the ^{13}C dimension and greatly alleviates peak overlapping. In $HSQC_0$ the cross-peaks intensities is proportional to concentration of individual metabolites, which can be converted to absolute concentrations by reference to an internal standard of known concentration. This technique has been applied to quantify individual compounds in complex natural mixtures, without isolation or purification. Thiocoraline **69** is a scarce example of a marine product that was selective quantified at a level of 1% (w/w) in an extract from a *Verrucosispora* sp. isolated from the sponge *Chondrilla caribensis* f. *caribensis* [90] (Figure 7.28). This compound has shown potent cytotoxicity against several cancer cell lines [91].

7.7 COMBINED NMR TECHNIQUES AND DIFFERENT FAMILIES OF COMPOUNDS

In this chapter we have described the most important NMR techniques used in the structural characterization of natural compounds from marine sources, always exemplified with the structural elucidation of specific bioactive marine products. Since these compounds present complex and not repetitive structures, making it not possible to compile their NMR characteristics by families, we will describe the full characterization of some derivatives using a combination of the described NMR techniques.

El-Amraoui *et al*. reported the structure elucidation of the antifungal haliscosamine **70** (Figure 7.29), a new sphisgosine derivative, isolated from the Moroccan marine sponge *Haliclona viscosa* [92]. The ^{1}H NMR spectrum revealed the presence of 45 protons in the range of 0.9 to 5.4 ppm, while the ^{13}C APT spectrum (the Attached Proton Test experiment is a common way to assign C-H multiplicities in ^{13}C NMR; the phase of CH and CH_3 peaks is 180° different from C and CH_2 peaks) combined with the HSQC spectrum identified 22 carbons (1 methyl, 15 methylene, and 6 methines) bounded to 39 protons. From

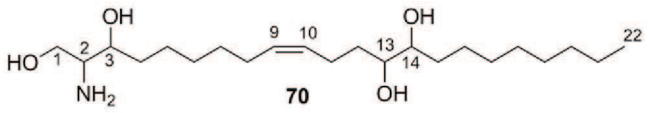

FIGURE 7.29 Structure of haliscosamine **70**.

these they have assigned the resonances of oxygenated carbons [59.1 (C-1), 67.7 (C-3), 73.4 (C-13), and 73.8 (C-14) ppm], a probably nitrogenated one [57.7 (C-2) ppm] and two double bounded carbons [129.1 (C-9) and 129.8 (C-10) ppm] (Table 7.1).

TABLE 7.1 NMR Spectroscopic Data of Haliscosamine 70 [92]

Position	δ ^{1}H ppm *J*(Hz)	δ ^{13}C ppm	HMBC	COSY	TOCSY
1a	3.67, dd, *J* 11.7, 4.0	59.1	2, 3	1b, 2, 3	2,3
1b	3.79, dd, *J* 11.7, 4.0		2, 3	1a, 2, 3	2, 3
2	3.07, m	57.7	1, 3, 4	1	1, 3
3	3.69, m	67.7	1, 2, 4, 5	1,4	1, 2, 4, 6
4a	1.47,m	33.5	2, 3, 5		
4b	1.57, m		2, 3, 5		
5a	1.40, m	24.9	3		
5b	1.57,m		3		
6	1.37, m	28.94			
7	1.37, m	29.45	8	8	9
8	2.09, m	26.7	7, 9	7, 9, 10	
9	5.39, m	129.1	8	8, 10	7, 8
10	5.40, m	129.8	11	8, 9, 11	11, 13
11a	2.13, m	23.3	10, 12, 13	10, 12	10, 13
11b	2.24, m		10, 12, 13	10, 12	10, 13
12a	1.54, m	32.6	11, 13		13
12b	1.59, m		11, 13		13
13	3.42	73.4	11, 12, 14, 15		10, 11, 12, 15
14	3.40	73.8	13, 15, 16	15	
15a	1.44, m	32.7	13, 14, 16	14	13
15b	1.54, m		13, 14, 16	14	13
16a	1.37, m	25.6	14, 15		
16b	1.52, m		14, 15		
17	1.37, m	29.17			
18	1.37, m	29.18			
19	1.37, m	29.20			
20	1.33, m	31.7	21, 22		
21	1.36, t, *J* 6.5	22.3	20, 22		
22	0.92	13.1	20, 21		

The referred data together with the high resolution mass spectrum indicate that the remaining six protons must be due to the presence of one NH_2 and four OH groups (this information could be confirmed running the ^1H NMR spectrum with some drops of D_2O).

The information given by the COSY, HMQC, HMBC, and TOCSY spectra allowed to assign three units of the structures C-1 to C-5, C-8 to C-16, and C-20 to C-22, but the connectivities between them were not possible due to the strong overlapping in the ^1H NMR spectrum. In order to solve this problem and to simplify the analysis of the spectrum, the authors performed an extensive study of ^1H–^1H decoupling experiments. (This experiment belongs to a class of experiments known as double-resonance experiments and offers a simple and effective means to identify coupled protons. The idea is to selectively saturate one multiplet in the spectrum with a radio-frequency during acquisition. This causes a loss of all couplings with the saturated proton and, hence, the multiplet structure of its partners will change.) These series of experiments allowed assembly of the entire structure of haliscosamine **70** (Figure 7.29).

Finally the (*Z*)-geometry of the double was established from a ^1H NMR of **70** acquired in CD_3OD with some drops of benzene, which increased the resolution in the vinylic part of the spectrum and allowed to determine the characteristic coupling constant value of 10 Hz. The small difference between the carbon resonances of C-8 (26.8 ppm) and C-11 (23.3 ppm) also confirms the stereochemistry of this double bond.

Jaspers *et al*. [93] described the discovery and structure elucidation of the cytotoxic laurefurenynes A-F **71-76** (Figure 7.30), cyclic ether acetogenins from the aqueous extract of the marine red alga *Laurencia* sp. The analysis of the ^1H and ^{13}C NMR spectra in $CDCl_3$ of laurefurenyne A **71** (Tables 7.2 and 7.3) revealed the presence of a C_{15} acetogenin, bearing one methyl group (belonging to an ethyl group), four methylenes, six oxygenated-sp^3 methines, two sp^2 methines, one sp methine, and a quaternary carbon. Based on the coupling constants and COSY and HSQC spectra it was possible to establish a *cis*-ene-yne moiety [6.06 (H-4, dt, *J* 10.9 and 7.9 Hz), 5.57 (H-3, dd, *J* 10.9 and 2.0 Hz), 3.10 (H-1, d, *J* 2.0 Hz); 139.9 (C-4), 111.3 (C-3), 80.0 (C-2), and 82.4 (C-1) ppm].

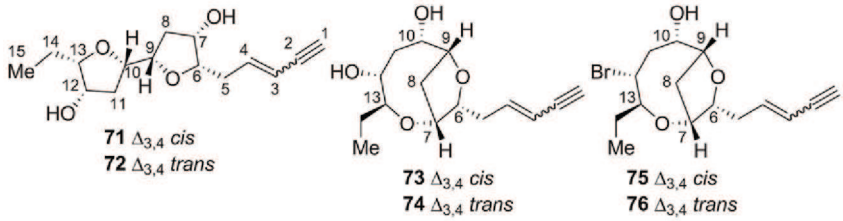

FIGURE 7.30 Structures of laurefurenynes A-F **71–76**.

TABLE 7.2 ^{1}H NMR Spectroscopic Data of Laurefurenynes A-F **71-76** [93]

Position	**71** δ ^{1}H ppm *J*(Hz)	**72** δ ^{1}H ppm *J*(Hz)	**73** δ ^{1}H ppm *J*(Hz)	**74** δ ^{1}H ppm *J*(Hz)	**75** δ ^{1}H ppm *J*(Hz)	**76** δ ^{1}H ppm *J*(Hz)
1	3.10, d, *J* 2.0	2.83, d, *J* 2.1	3.09, d, *J* 2.1	2.76, d, *J* 1.6	3.07, d, *J* 2.0	2.79, d, *J* 1.7
2	—	—	—	—	—	—
3	5.57, dd, *J* 10.9, 2.0	5.58, dd, *J* 15.5, 2.1	5.55, dd, *J* 11.2, 2.1	5.59, dd, *J* 16.0, 1.6	5.51, dd, *J* 10.9, 2.0	5.55, dd, *J* 15.9, 1.7
4	6.05, dt, *J* 10.9, 7.9	6.22, dt, *J* 15.5, 7.6	6.08, dt, *J* 11.2, 8.0	6.26, dt, *J* 16.0, 7.5	6.01, dt, *J* 10.9, 7.8	6.18, dt, *J* 15.9, 7.5
5a	2.61, m	2.44, m	2.85, m	2.54, m	2.79, m	2.56, m
5b		2.37, m	2.69, m		2.68, m	2.45, m
6	3.90, ddd, *J* 10.1, 6,5, 3.8	3.90, ddd, *J* 10.2, 6.6, 3.7	3.87, m	3.73, m	3.72, ddd, *J* 8.8, 7.1, 2.0	3.67, ddd, *J* 8.6, 7.3, 2.1
7	4.12, m	4.10, m	4.02, m	3.99, dd, *J* 3.6, 2.0	3.94, m	3.94, m
8a	1.86, m	1.85, m	2.98,d, *J* 15.2	3.02, d, *J* 16.2	2.24, m	2.24, d, *J* 16.1
8b	1.69, m	1.68, m	1.96, m	1.93, m	1.92, m	1.92, m
9	4.37, m	4.40, m	4.30, m	4.29, dd, *J* 9.8, 3.9	4.10,dd, *J* 9.6, 4.0	4.10, dd, *J* 9.6, 3.9
10	4.14, m	4.16, m	4.09, m	4.07, m	3.96, m	3.96, m
10-OH	—	—	3.34, br s	3.37, br s	—	—
11a	2.19, m	2.20, m	2.21, m	2.20, m	3.01, dddd, *J* 15.3, 11.3, 9.7, 1.8	2.98, dddd, *J* 15.4, 11.2, 9.8, 1.8
11b	1.81, dd, *J* 14.5, 3.1	1.79, dd, *J* 13.9, 3.0			2.28, dd, *J* 15.2, 5.1	2.28, dd, *J* 15.1, 5.0
12	3.98, dd, *J* 5.1, 2.3	4.01, dd, *J* 5.5, 2.3	4.29, m	4.30, m	4.55, t, *J* 9.6	4.54, t, *J* 9.6
12-OH	—	—	2.72, br s	2.80, br s		
13	3.49, ddd, *J* 13.6, 6.8, 2.4	3.52, ddd, *J* 9.4, 6.9, 2.4	3.81, m	3.76, m	3.86, ddd, *J* 11.8, 9.6, 2.8	3.84, ddd, *J* 13.5, 9.6, 2.4
14	1.66, m	1.69, m	1.74, m, 1.57, m	1.77, m, 1.57, m	1.93, m, 1.66, m	1.96, m, 1.65, m
15	0.94, t, *J* 7.5	0.97, t, *J* 7.5	1.01, t, *J* 7.5	0.98, t, *J* 7.5	1.02, t, *J* 7.2	1.01, t, *J* 7.2

TABLE 7.3 ^{13}C NMR Spectroscopic Data of Laurefurenynes A–F **71–76** [93]

Position	**71** δ ^{13}C ppm	**72** δ ^{13}C ppm	**73** δ ^{13}C ppm	**74** δ ^{13}C ppm	**75** δ ^{13}C ppm	**76** δ ^{13}C ppm
1	82.4	76.7	81.9	76.2	81.7	76.6
2	80.0	81.7	—	82.2	80.7	81.8
3	111.3	112.0	110.0	110.8	110.2	111.3
4	139.9	140.7	141.8	142.5	141.5	142.1
5	34.1	37.1	30.4	32.8	30.1	32.8
6	85.7	85.4	83.0	82.9	83.2	83.4
7	74.8	74.9	71.0	70.2	70.2	70.1
8	37.1	37.3	32.0	31.7	33.1	33.2
9	79.1	79.1	79.5	79.7	78.6	78.4
10	78.2	78.1	73.3	73.4	70.5	70.5
11	34.5	34.5	30.8	29.7	38.8	38.9
12	70.8	70.8	72.8	73.1	51.8	51.8
13	85.6	85.7	78.9	79.3	83.2	83.5
14	21.8	21.8	23.1	22.3	23.1	23.2
15	10.5	10.8	11.3	11.4	11.8	11.9

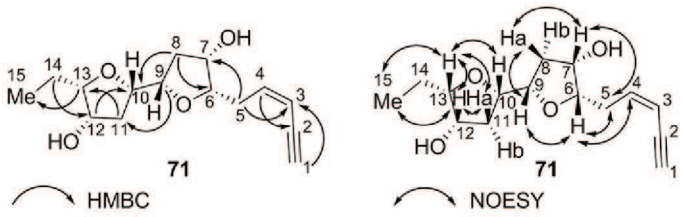

FIGURE 7.31 Main HMBC and NOESY correlations of laurefurenyne A **71**.

The combined analysis of the COSY, selective 1D TOCSY and HSQC spectra established a continuous chain of carbon atoms (C-1 to C-15) of the C_{15} acetogenin, which was confirmed by the HMBC correlations (Figure 7.31). In order to circumvent some doubts around the two ether bridges of the structure due to an extensive overlapping of signals, the authors acquired the ^{1}H NMR spectrum of laurefurenyne A **71** in DMSO-d_6, which combined with a new COSY spectrum allowed the location of the two hydroxyl groups at C-7 and C-12.

Since there were three possible carbon frameworks, a deep analysis of the carbon chemical shifts led to the proposal of a central 2,2′-bifuran skeleton. The stereochemistry around the two tetrahydrofuran rings was established by a 2D NOESY spectrum (Figure 7.31). The relative stereochemistry of the two tetrahydrofuran rings was difficult and needed some modeling, which confirmed the strong NOE correlations of H-9 with both H-10 and H-11. Thus the relative stereochemistry of laurefurenyne A **71** was assigned as (6*S**,7*S**,9*S**,10*S**,12*S**,13*S**).

The ^{1}H and ^{13}C NMR spectra of laurefurenyne A **71** and B **72** were very similar (Tables 7.2 and 7.3), except for the coupling constant of the vinylic system (*J* 15.5 Hz) of **72**, which is consistent with a *trans*-configuration consistent with a *trans*-ene-yne moiety.

The presence of a *cis*-ene-yne moiety of laurefurenyne C **73** was easily detected as was laurefurenyne A **71** (Table 7.2). The C1-C15 contiguous spin system was inferred from a deep analysis of the COSY and HSQC spectra of laurefurenyne C **73** acquired in both $CDCl_3$ and DMSO-d_6 due to strong signal overlapping, but the two hydroxyl groups in this case were located at C-10 and C-12. This was confirmed by a selective 1D TOCSY experiment as well as by HMBC correlations, which allows the establishment of the new location of one of the ether linkages to C7-C13 (H-7 → C-13) and leaving the other ether bridge in the C6-C9 carbons. Thus the carbon skeleton of laurefurenyne C **73** was identified as a 2,8-dioxabicyclo[5.2.1]decane. Once again, the stereochemistry of the stereogenic centers of this laurefurenyne C **73** was established by 2D NOESY experiments (NOE cross-peaks of H-8 with H-6, H-7, H-9; of H-8a with H-7, H-10, H-11b, H-12, H-14; and of H-7 with H-15) and assigned as (6*R**,7*R**,9*R**,10*S**,12*R**,13*S**).

The structural difference of laurefurenyne D **74** relatively to the C derivative was only the stereochemistry of their vinylic system, which was identified by the characteristic coupling constant (*J* 16.0 Hz) of a *trans*-configuration. All the other spectroscopic data (Tables 7.2 and 7.3) and 2D NOESY correlations of laurefurenyne D **74** were very similar to those of laurefurenyne C **73**.

The high resolution mass spectra (HRMS) of laurefurenynes E **75** and F **76** revealed that a bromine replaced an hydroxyl group in the structure of the corresponding laurefurenynes C **73** and D **74**, while the ^{1}H and ^{13}C NMR indicate that it was the 12α-hydroxyl group replaced by a 12α-bromine substituent (Tables 7.2 and 7.3).

Four antimicrobial fatty acids, ieodomycins A-D **77-80** (Figure 7.32) [94], have been isolated from the ethyl acetate extract of a culture of a marine *Bacillus* sp. The UV spectrum of **77** indicated the presence of a conjugated diene, while the IR revealed the presence of hydroxyl and ester carbonyl groups. The ^{1}H, ^{13}C NMR, and HSQC spectra of ieodomycin A **77** showed four vinylic carbons (115.1–140.1 ppm), including a terminal vinylic methylene (115.1 ppm), two oxygenated methines, two methyls, one of them oxygenated, and an ester

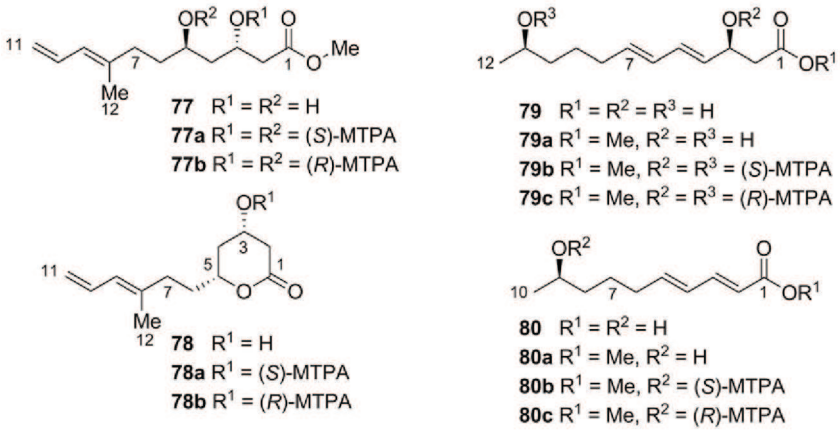

FIGURE 7.32 Structures of ieodomycins A–D **77–80** and their corresponding MTPA esters.

carbonyl carbon (Tables 7.4 and 7.5). The COSY spectrum indicated two isolated spin systems (H-2 to H-7 and H-9 to H-11), their connectivity being established through the HMBC correlations (H-7 → C-8 and C-9) (Figure 7.33). The other HMBC correlations confirmed all the other connectivities of ieodomycin A **77**. The ROESY correlations of H-10 with H-12 and of H-9 with H-11b establishes the (*E*)-stereochemistry of the C8=C9 double bond (Figure 7.33). The carbon resonances of C-3 and C-5 are consistent with an *anti*-arrangement of the 1,3-diol model system, according to the Kishi's Universal NMR Database [41,42] (Figure 7.34). Moreover the absolute configuration was established by the modified Mosher's method, preparing the esters (*S*)-MTPA-**77a** and (*R*)-MTPA-**77b** starting from ieodomycin A **77** (Figure 7.34). The negative values of $\Delta\delta^{SR}$ of H-3 (–0.11 ppm), H-4 (–0.12/-0.13 ppm), and H-5 (–0.17 ppm) correspond to an *anti*-1,3-diols [95], indicating a (3*S*,5*R*) configuration. Thus the structure of ieodomycin A **77** was established as (3*S*,5*R*,8*E*)-methyl 3,5-dihydroxy-8-methylundeca-8,10-dienoate.

The spectroscopic data (^{1}H, ^{13}C NMR, and HRMS) of ieodomycin B **78** were very similar to those of ieodomycin A **76**, but having one less carbon, four hydrogens, and one oxygen atom. The comparison of ^{1}H and ^{13}C NMR spectra of **77** and **78** revealed that the latter does not have the methoxyl group and its C-1 was attached to the oxygen at C-5, forming a δ-lactone ring (Figure 7.32; Tables 7.4 and 7.5). The configuration of ieodomycin B **78** was assigned based on the ^{1}H–^{1}H coupling constants and ROESY correlations, which suggested a chair conformation for the δ-lactone ring (Figure 7.33). The absolute configuration was also established by application of the modified Mosher's method, which indicate a (3*S*)-configuration (Figure 7.34). The (5*R*)-configuration was established based on the ROE cross-peaks observed in the ROESY spectrum that indicate an *anti*-relationship between C-3 and C-5. All the spectroscopic data support the structure of ieodomycin B **78** as

TABLE 7.4 ^{1}H NMR Spectroscopic Data of Ieodomycins A–D **77–80** [94]

Position	**77** δ ^{1}H ppm *J*(Hz)	**78** δ ^{1}H ppm *J*(Hz)	**79** δ ^{1}H ppm *J*(Hz)	**80** δ ^{1}H ppm *J*(Hz)
1				
2	2.47, dd, *J* 10.0, 5.0	2.36, dd, *J* 16.8, 7.3 (H-2ax)	2.45, d, *J* 6.0	5.78, d, *J* 15.3
		2.86, dd, *J* 16.8, 1.3 (H-2eq)		
3	4.25, m	4.19, dddd, *J* 10.4, 7.3, 3.5, 1.3 (H-3ax)	4.50, m	7.21, dd, *J* 15.3, 10.5
4	1.52, m	2.24, ddd, *J* 13.5, 10.4, 7.3 (H-4ax)	5.60, dd, *J* 15.3, 6.5	6.24, dd, *J* 15.3, 10.5
		2.27, ddd, *J* 13.5, 4.2, 3.5 (H-4eq)		
5	3.76, m	4.24, dddd, *J* 10.4, 7.3, 4.2, 3.5 (H-5ax)	6.22, dd, *J* 15.3, 10.5	6.16, m
6	1.56, m	1.80, m	6.03, dd, *J* 15.3, 10.5	2.20, m
7	2.10, m	2.18, m	5.70, dt, *J* 15.3, 7.0	1.45, m
	2.19, m	2.25, m		1.56, m
8			2.10, m	1.43, m
9	5.86, d, *J* 10.5	5.88, d, *J* 10.6	1.38, m	3.72, m
10	6.57, ddd, *J* 16.7, 10.5, 10.5	6.58, ddd, *J* 16.6, 10.6, 10.6	1.50, m	1.14, d, *J* 6.0
11	4.93, d, *J* 10.5 (H-11b)	4.96, dd, *J* 10.6, 2.2, (H-11b)	1.42, m	
	5.04, d, *J* 16.7 (H-11a)	5.07, dd, *J* 16.6, 2.2 (H-11a)	3.70, m	
12	1.75, s	1.77, s	1.13, d, *J* 6.0	
OMe	3.67, s			

TABLE 7.5 ^{13}C NMR Spectroscopic Data of Ieodomycins A–D **77–80** [94]

Position	**77** δ ^{13}C ppm	**78** δ ^{13}C ppm	**79** δ ^{13}C ppm	**80** δ ^{13}C ppm
1	174.0	174.1	175.6	171.5
2	43.9	40.2	43.7	121.3
3	66.6	64.4	70.2	146.5
4	45.3	38.7	133.6	130.0
5	68.8	78.5	132.1	145.3
6	37.5	34.9	131.0	34.0
7	37.0	36.1	136.1	26.2
8	140.1	139.0	33.7	39.7
9	127.0	127.6	26.7	68.4
10	134.7	134.5	39.8	23.6
11	115.1	115.6	68.5	
12	16.8	16.6	23.6	
OMe	52.1			

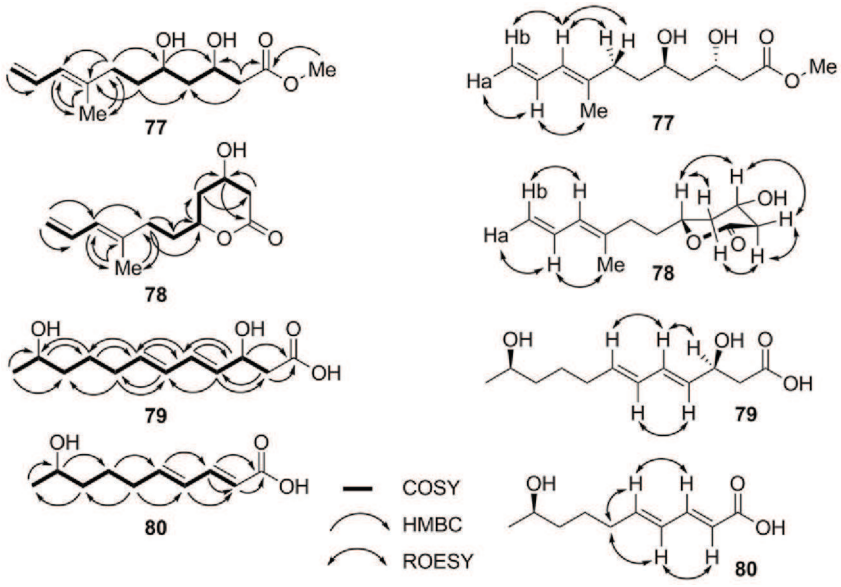

FIGURE 7.33 Main COSY, HMBC, and ROESY correlations of ieodomycins A–D **77–80**.

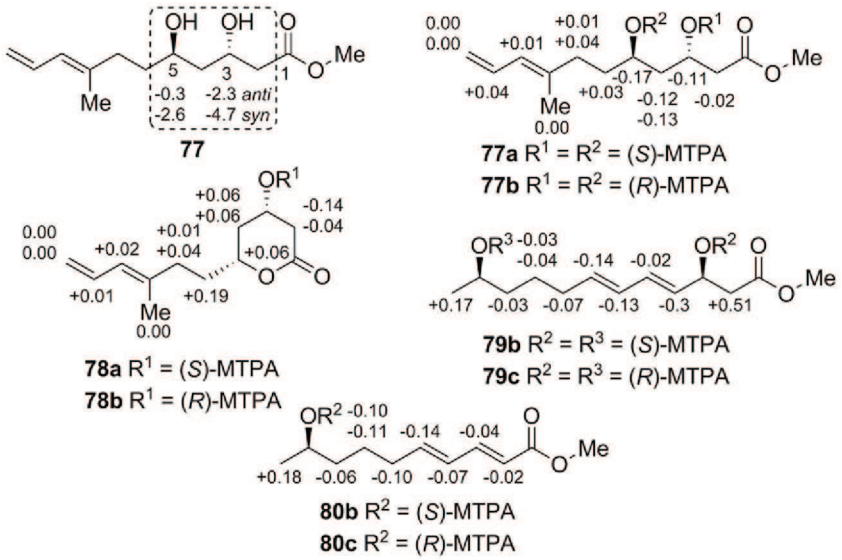

FIGURE 7.34 The $\Delta\delta^{SR}$ data for the MTPA esters of ieodomycins A–D **77–80**.

(3*S*,5*R*,8*E*)-3-hydroxy-5-(8-methylhexa-8,10-dienyl)tetrahydro-1*H*-pyran-1-one (Figures 7.33 and 7.34).

The COSY spectrum of ieodomycin C **79** indicates a single spin system from H-2 to H-12, while the (*E*)-configuration of both vinylic systems was based on the characteristic scalar coupling constants (both *J* 15.3 Hz), although also confirmed by the ROESY correlations (H-4 → H-6 and H-5 → H-7). All the proton and carbon resonances were then assigned through the analysis of their ^{1}H, ^{13}C, HSQC, and HMBC spectra (Figure 7.33; Tables 7.4 and 7.5). The synthesis of the modified Mosher's diesters and the analysis of the $\Delta\delta^{SR}$ values assigns the configuration of C-3 and C-11 as (*S*) and (*R*), respectively (Figure 7.34). Thus ieodomycin C **79** was identified as (3*S*,4*E*,6*E*,11*R*)-3,11-dihydroxydodeca-4,6-dienoic acid.

The analysis of the spectroscopic data (^{1}H, ^{13}C NMR, and HRMS) of ieodomycin D **80** shows that this structure has two carbons, four hydrogens, and one oxygen less than ieodomycin C **79** (Tables 7.4 and 7.5). Like in the case of **79**, the COSY spectrum of ieodomycin D **80** revealed the presence of only one spin system, the (*E*)-configurations of their vinylic systems were based on the large ^{1}H–^{1}H coupling constants (both *J* 15.3 Hz) and confirmed by ROESY correlations, the carbon resonances were assigned based on the HSQC correlations, while the carbon skeleton was established by the HMBC connectivities (Figure 7.33). The (9*S*)-absolute configuration was assigned by the modified Mosher's method (Figure 7.34). Thus the structure of ieodomycin D **80** was unambiguously established as (2*E*,4*E*,9*R*)-9-hydroxydeca-2,4-dienoic acid.

7.8 REVISED STRUCTURES

Despite all the development in the spectroscopic techniques, including those of the NMR experiments described in this chapter and the detailed modern spectral analyses, the sad truth is that structures of natural products and also those of marine sources originally proposed based on these techniques and analyses often include misassignments. There were two articles on natural products' structural revisions covering the periods 1990 to 2005 [96] and 2005 to 2009 [97] where they focused the application of chemical (particularly total) synthesis to structure elucidation, including terrestrial and marine-derived metabolites.

In a more recent review, McPhail *et al*. [98] surveyed marine natural products structural revision based on spectroscopic and chemical synthesis. This covers the period of 2005 to 2010 and identifies the techniques used in the misassignment of all the structures revised during this period, most notably that the NOE experiments (NOE difference, NOESY, and ROESY) and the NMR comparison are responsible for around half of these misassignments. The high frequency of NOE associated errors implies that configurational misassignments predominate over constitutional errors. The source of misassignments of marine natural products can be divided into the subcategories constitution errors and configuration errors, described as follows.

Constitution errors include cyclization (e.g., five- vs six-membered cycles; differentiation of fused six-membered from two five-membered rings linked by a single bond), regioisomerism (e.g., placement of substituents on cycles), substituent identity (e.g., identity of heteronuclear substituents, based on MS techniques and subject to errors depending on the substituent stability and the ionization technique used), hydrocarbon chains (e.g., a challenge topic of the MS technique based on the molecular ion and fragmentation patterns), and symmetry of dimerization (based on incorrect formula).

Configuration errors are those such as absolute and relative configuration. Generally, in the case of absolute configuration it is necessary to perform chemical degradation and/or derivatization followed by comparison of chromatographic retention and spectroscopic properties with a standard of model compounds. Since the isolation quantity of marine natural products is generally very small, the spectroscopic comparison of the new metabolites with known assigned compounds to extrapolate absolute configuration is common and can lead to propagation of errors. Mosher's analyses rely on the application of empirically derived principles and consequently errors can be sustained and propagated. Taking into account all these errors and their origin, with a sufficient sample, X-ray crystallography can be considered a gold standard for assignment of absolute configuration, but when there is a very small amount of sample, the errors can almost exclusively await detection and revision by total synthesis. The NOE data are responsible for the majority of the relative configuration misassignments of marine natural products. This situation highlights the need for a careful evaluation of all the molecular models that are consistent with NOE constraints, which support the use of computational modeling for this analysis.

Considering the sources of misassignments leads to the question of how these errors are detected and which techniques are used to revise the corresponding structure. Nondestructive and relatively sensitive NMR methods, although the greatest source of misassignments, still provide the major contribution to marine natural products revision, immediately followed by total and partial synthesis.

The increasingly high-field magnets and sensitive probes do not necessarily attenuate the rate of structural misassignments, since they are still to be reported [e.g., 99,100], but they permit the attempted structure elucidation of increasingly limited quantities of minor components from natural products extracts, as well as larger molecules of greater structural complexity. Although total syntheses of marine natural products require extremely high-level work in organic chemistry, it will surely continue to be central to the confirmation of natural product structure assignment [e.g., 101,102], as well as providing material for biological testing toward pharmaceutical development, and investigations of biosynthetic pathways.

ACKNOWLEDGEMENTS

The authors acknowledge University of Aveiro, Fundação para a Ciência e Tecnologia (FCT, Portugal), European Union, QREN, FEDER, and COMPETE for funding the QOPNA Research Unit.

REFERENCES

[1] K. Sugahara, Y. Kitamura, M. Murata, M. Satake, K. Tachibana, J. Org. Chem. 76 (2011) 3131–3138.
[2] G. Fan, Z. Li, S. Shen, Y. Zeng, Y. Yang, M. Xu, T. Bruhn, H. Bruhn, J. Morschhäuser, G. Bringmann, W. Lin, Bioorg. Med. Chem. 18 (2010) 5466–5474.
[3] T. Hertiani, R. Edrada-Ebel, S. Ortlepp, R.W.M. van Soest, N.J. de Voogd, V. Wray, U. Hentschel, S. Kozytska, W.E.G. Müller, P. Proksch, Bioorg. Med. Chem. 18 (2010) 1297–1311.
[4] H. Yamazaki, H. Rotinsulu, T. Kaneko, K. Murakami, H. Fujiwara, K. Ukai, M. Namikoshi, Mar. Drugs 10 (2012) 2691–2697.
[5] S. Sato, F. Iwata, S. Yamada, M. Katayama, J. Nat. Prod. 75 (2012) 1974–1982.
[6] B. Ohlendorf, D. Schulz, A. Erhard, K. Nagel, J.F. Imhoff, J. Nat. Prod. 75 (2012) 1400–1404.
[7] P.D. Boudreau, T. Bryum, W.-T. Liu, P.C. Dorrestein, W.H. Gerwick, J. Nat. Prod. 75 (2012) 1560–1570.
[8] W.M. Abdel-Mageed, B.F. Milne, M. Wagner, M. Schumacher, P. Sandor, W. Pathom-aree, M. Goodfellow, A.T. Bull, K. Horikoshi, R. Ebel, M. Diederich, H.-P. Fiedler, M. Jaspars, Org. Biomol. Chem. 8 (2010) 2352–2362.
[9] D.-G. Kim, K. Moon, S.-H. Kim, S.-H. Park, S. Park, S.K. Lee, K.-B. Oh, J. Shin, D.-C. Oh, J. Nat. Prod. 75 (2012) 959–967.
[10] A. Plaza, J.L. Keffer, G. Bifulco, J.R. Lloyd, C.A. Bewley, J. Am. Chem. Soc. 132 (2010) 9069–9077.

[11] S. Mo, A. Krunic, B.D. Santarsiero, S.G. Franzblau, J. Orjala, Phytochemistry 71 (2010) 2116–2123.
[12] L.A. Salvador, V.J. Paul, H. Luesch, J. Nat. Prod. 73 (2010) 1606–1609.
[13] R. Finlayson, A.N. Pearce, M.J. Page, M. Kaiser, M.-L. Bourguet-Kondracki, J.L. Harper, V.L. Webb, B.R. Copp, J. Nat. Prod. 74 (2011) 888–892.
[14] I. Djinni, A. Defant, M. Kecha, I. Mancini, Mar. Drugs 11 (2013) 124–135.
[15] K. Chakraborty, A.P. Lipton, R. Paulraj, R.D. Chakraborty, Eur. J. Med. Chem. 45 (2010) 2237–2244.
[16] S. Li, M. Wei, G. Chen, Y. Lin, Chem. Nat. Comp. 48 (2012) 371–373.
[17] J. Wiese, B. Ohlendorf, M. Blümel, R. Schmaljohann, J.F. Imhoff, Mar. Drugs 9 (2011) 561–585.
[18] C. Li, J. Zhang, C. Shao, W. Ding, Z. She, Y. Lin, Chem. Nat. Comp. 47 (2011) 382–384.
[19] Y. Chen, J. Pan, F. Xu, F. Liu, J. Yang, C. Huang, C. Xu, Y. Lu, X. Cai, Z. She, Y. Lin, Chem. Nat. Comp. 46 (2010) 230–232.
[20] F. Alihosseini, J. Lango, K.-S. Ju, B.D. Hammock, G. Sun, Biotechnol. Prog. 26 (2010) 352–360.
[21] F. Song, H. Dai, Y. Tong, B. Ren, C. Chen, N. Sun, X. Liu, J. Bian, M. Liu, H. Gao, H. Liu, X. Chen, L. Zhang, J. Nat. Prod. 73 (2010) 806–810.
[22] J. You, H. Dai, Z. Chen, G. Liu, Z. He, F. Song, X. Yang, H. Fu, L. Zhang, X. Chen, J. Ind. Microbiol. Biotechnol. 37 (2010) 245–252.
[23] R.H. Jiao, H. Xu, J.T. Cui, H.M. Ge, R.X. Tan, J. Appl. Microbiol. 114 (2013) 1046–1053.
[24] R. Finlayson, A. Brackovic, A. Simon-Levert, B. Banaigs, R.F. O'Toole, C.H. Miller, B.R. Copp, Tetrahedron Lett. 52 (2011) 837–840.
[25] H.B. Park, H.O. Yang, K.R. Lee, H.C. Kwon, Molecules 16 (2011) 3519–3529.
[26] S. Felder, S. Dreisigacker, S. Kehraus, E. Neu, G. Bierbaum, P.R. Wright, D. Menche, T.F. Schäberle, G.M. König, Chem. Eur. J. 19 (2013) 9319–9324.
[27] N. Liu, F. Shang, L. Xi, Y. Huang, Mar. Drugs 11 (2013) 1524–1533.
[28] F.-Z. Wang, Z. Huang, X.-F. Shi, Y.-C. Chen, W.-M. Zhang, X.-P. Tian, J. Li, S. Zhang, Bioorg. Med. Chem. Lett. 22 (2012) 7265–7267.
[29] K. Tidgewell, N. Engene, T. Byrum, J. Media, T. Doi, F.A. Valeriote, W.H. Gerwick, ChemBioChem 11 (2010) 1458–1466.
[30] Y. Zhou, A. Mándi, A. Debbab, V. Wray, B. Schulz, W.E.G. Müller, W. Lin, P. Proksch, T. Kurtán, A.H. Aly, Eur. J. Org. Chem. (2011) 6009–6019.
[31] Y. Zhou, A. Debbab, A. Mándi, V. Wray, B. Schulz, W.E.G. Müller, M. Kassack, W. Lin, T. Kurtán, P. Proksch, A.H. Aly, Eur. J. Org. Chem. (2013) 894–906.
[32] W. Xin, X. Ye, S. Yu, X.-Y. Lian, Z. Zhang, Mar. Drugs 10 (2012) 2388–2402.
[33] Y.-B. Cheng, P.R. Jensen, W. Fenical, Eur. J. Org. Chem. (2013) 3751–3757.
[34] F. Cen-Pacheco, J.A. Villa-Pulgarin, F. Mollinedo, M. Norte, A.H. Daranas, J.J. Fernández, Eur. J. Med. Chem. 46 (2011) 3302–3308.
[35] W. Wang, H. Kim, S.-J. Nam, B.J. Rho, H. Kang, J. Nat. Prod. 75 (2012) 2049–2054.
[36] N. Matsumori, D. Kaneno, M. Murata, H. Nakamura, K. Tachibana, J. Org. Chem. 64 (1999) 866–876.
[37] D. Menche, Nat. Prod. Rep. 25 (2008) 905–918.
[38] Y. Kobayashi, J. Lee, K. Tezuka, Y. Kishi, Org. Lett. 1 (1999) 2177–2180.
[39] Y. Kobayashi, J. Lee, K. Tezuka, Y. Kishi, Org. Lett. 1 (1999) 2181–2184.
[40] Y. Kobayashi, C.-H. Tan, Y. Kishi, Helv. Chim. Acta 83 (2000) 2562–2571.
[41] Y. Kobayashi, C.-H. Tan, Y. Kishi, J. Am. Chem. Soc. 123 (2001) 2076–2078.

[42] S. Higabayashi, W. Czechtizky, Y. Kobayashi, Y. Kishi, J. Am. Chem. Soc. 125 (2003) 14379–14393.
[43] E. Fleury, M.-I. Lannou, O. Bistri, F. Sautel, G. Massiot, A. Pancrazi, J. Ardisson, Eur. J. Org. Chem. (2009) 4992–5001.
[44] J.M. Seco, E. Quiñoá, R. Riguera, Chem. Rev. 104 (2004) 17–117.
[45] J.M. Seco, E. Quiñoá, R. Riguera, Chem. Rev. 112 (2012) 4603–4641.
[46] J.A. Dale, H.S. Mosher, J. Am. Chem. Soc. 95 (1973) 512–519.
[47] G.R. Sullivan, J.A. Dale, H.S. Mosher, J. Org. Chem. 38 (1973) 2143–2147.
[48] N. Harada, Chirality 20 (2008) 691–723.
[49] W.S. Borges, G. Mancilla, D.O. Guimarães, R. Durán-Patrón, I.G. Collado, M.T. Pupo, J. Nat. Prod. 74 (2011) 1182–1187.
[50] M. Takahashi, K. Koyama, S. Natori, Chem. Pharm. Bull. 38 (1990) 625–628.
[51] S.J. Nam, S.P. Gaudêncio, C.A. Kauffman, P.R. Jensen, T.P. Kondratyuk, L.E. Marler, J.M. Pezzuto, W. Fennical, J. Nat. Prod. 73 (2010) 1080–1086.
[52] D.H. Marchbank, F. Berrue, R.G. Kerr, J. Nat. Prod. 75 (2012) 1289–1293.
[53] D. Lai, Y. Li, M. Xu, Z. Deng, L. van Ofwegen, P. Qian, P. Proksch, W. Lin, Tetrahedron 67 (2011) 6018–6029.
[54] L.G. Meimetis, D.E. Williams, N.R. Mawji, C.A. Banuelos, A.A. Lal, J.J. Park, A.H. Tien, J.G. Fernandez, N.J. de Voogd, M.D. Sadar, R.J. Andersen, J. Med. Chem. 55 (2012) 503–514.
[55] T. Conroy, J.T. Guo, R.G. Linington, N.H. Hunt, R.J. Payne, Chem. Eur. J. 17 (2011) 13544–13552.
[56] T.A.M. Gulder, H. Hong, J. Correa, E. Egereva, J. Wiese, J.F. Imhoff, H. Gross, Mar. Drugs 10 (2012) 2912–2935.
[57] A.R. Carroll, G. Pierens, G. Fechner, P.A. Leone, A. Ngo, M. Simpson, J.N.A. Hooper, S.-L. Boström, D. Musil, R.J. Quinn, J. Am. Chem. Soc. 124 (2002) 13340–13341.
[58] S. Hanessian, R. Margarita, A. Hall, S. Johnstone, M. Tremblay, L. Parlanti, J. Am. Chem. Soc. 124 (2002) 13342–13343.
[59] A.D. Rodríguez, E. González, S.D. Huang, J. Org. Chem. 63 (1998) 7083–7091.
[60] T.J. Heckrodt, J. Mulzer, J. Am. Chem. Soc. 125 (2003) 4680–4681.
[61] H. Miyaoka, D. Honda, H. Mitome, Y. Yamada, Tetrahedron Lett. 43 (2002) 7773–7775.
[62] K. Ota, T. Kurokawa, E. Kawashima, H. Miyaoka, Mar. Drugs 7 (2009) 654–671.
[63] S.C. Bobzin, S. Yang, T.P. Kasten, J. Chromatogr. B 748 (2000) 259–267.
[64] S.C. Bobzin, S. Yang, T.P. Kasten, J. Ind. Microbiol. Biotecnhol. 25 (2000) 342–345.
[65] R.A. Edrada, M. Heubes, G. Brauers, V. Wray, A. Berg, U. Gräfe, M. Wohlfarth, J. Mühlbacher, K. Schaumann, Sudarsono, G. Bringmann, P. Proksch, J. Nat. Prod. 65 (2002) 1598–1604.
[66] G. Bringmann, G. Lang, S. Steffens, E. Günther, K. Schaumann, Phytochemistry 63 (2003) 437–443.
[67] R. Brkljača, S. Urban, J. Liq. Chromatogr. Rel. Technol. 34 (2011) 1063–1076.
[68] D.A. Dias, S. Urban, J. Sep. Sci. 32 (2009) 542–548.
[69] D.A. Dias, J.M. White, S. Urban, Nat. Prod. Commun. 4 (2009) 157–172.
[70] D.A. Dias, S. Urban, Phytochemistry 72 (2011) 2081–2089.
[71] M.A. Timmers, D.A. Dias, S. Urban, Mar. Drugs 10 (2012) 2089–2102.
[72] S. Urban, M.A. Timmers, Nat. Prod. Commun. 8 (2013) 715–719.
[73] Z. Yang, J. Pharm. Biomed. Anal. 40 (2006) 516–527.
[74] J.W. Jaroszewski, Planta Med. 71 (2005) 795–802.
[75] L. Fremlin, M. Farrugia, A.M. Piggott, Z. Khalil, E. Lacey, R.J. Capon, Org. Biomol. Chem. 9 (2011) 1201–1211.

[76] M.L. Martin, J.-J. Delpuech, G.J. Martin, Practical NMR Spectroscopy, Heyden, London, (1980).
[77] C. Szántay Jr., Trends Anal. Chem. 11 (1992) 332–344.
[78] G.F. Pauli, B.U. Jaki, D.C. Lankin, J. Nat. Prod. 68 (2005) 133–149.
[79] G.F. Pauli, T. Gödecke, B.U. Jaki, D.C. Lankin, J. Nat. Prod. 75 (2012) 834–851.
[80] C.H. Cullen, G.J. Ray, C.M. Szabo, Magn. Reson. Chem. 51 (2013) 705–713.
[81] I.W. Burton, M.A. Quilliam and J.A. Walter, 42nd Experimental Nuclear Magnetic Resonance Spectroscopy Conference (ENC): Orlando, Florida, March 11-16, 2001.
[82] I.W. Burton, M.A. Quilliam, J.A. Walter, Anal. Chem. 77 (2005) 3123–3131.
[83] R. Perez, N. Rehmann, S. Crain, P. LeBlanc, C. Craft, S. MacKinnon, K. Reeves, I.W. Burton, J.A. Walter, P. Hess, M.A. Quiliam, J.E. Melanson, Anal. Bioanal. Chem. 398 (2010) 2243–2252.
[84] J.L. Carballo, B. Yañez, E. Zubía, M.J. Ortega, C. Vega, Mar. Biotechnol. 12 (2010) 516–525.
[85] D.M. Wilson, M. Puyana, W. Fenical, J.R. Pawlik, J. Chem. Ecol. 25 (1999) 2811–2823.
[86] T.F. Molinski, Curr. Opin. Biotechnol. 21 (2010) 819–826.
[87] D.S. Dalisay, T.F. Molinski, J. Nat. Prod. 72 (2009) 739–744.
[88] T.F. Molinski, Nat. Prod. Rep. 27 (2010) 321–329.
[89] K. Hu, W. Westler, J.L. Markley, J. Am. Chem. Soc. 133 (2011) 1662–1665.
[90] K. Hu, T.P. Wyche, T.S. Bugni, J.L. Markley, J. Nat. Prod. 74 (2011) 2295–2298.
[91] A. Negri, E. Marco, V. García-Hernández, A. Domingo, A.L. Llamas-Saiz, S. Porto-Sandá, R. Riguera, W. Laine, M.-H. David-Cordonnier, C. Bailly, L.F. García-Fernández, J.J. Vaquero, F. Gago, J. Med. Chem. 50 (2007) 3322–3333.
[92] B. El-Amraoui, J.-F. Biard, A. Fassouane, SpringerPlus 2 (2013) 252–271.
[93] W.M. Abdel-Mageed, R. Ebel, F.A. Valeriote, M. Jaspars, Tetrahedron 66 (2010) 2855–2862.
[94] M.A.M. Mondol, J.H. Kim, M. ah Lee, F.S. Tareq, H.-S. Lee, Y.-J. Lee, H.J. Shin, J. Nat. Prod. 74 (2011) 1606–1612.
[95] F. Freire, J.M. Seco, Q. Emilio, R. Riguera, J. Org. Chem. 70 (2005) 3778–3790.
[96] K.C. Nicolaou, S.A. Snyder, Angew. Chem. Int. 44 (2005) 1012–1044.
[97] M.E. Maier, Nat. Prod. Rep. 26 (2009) 1105–1124.
[98] T.L. Suyama, W.H. Gerwick, K.L. McPhail, Bioorg. Med. Chem. 19 (2011) 6675–6701.
[99] F. Zhu, G.Y. Chen, J. Wu, J. Pan, Nat. Prod. Res. 27 (2013) 1960–1964.
[100] J.W. Cha, J.-S. Park, T. Sim, S.-J. Nam, H.C. Kwon, J.R. Del Valle, W. Fenical, J. Nat. Prod. 75 (2012) 1648–1651.
[101] S. Das, R.K. Goswami, J. Org. Chem. 78 (2013) 7274–7280.
[102] M. Ebine, M. Kanemoto, Y. Manabe, Y. Konno, K. Sakai, N. Matsumori, M. Murata, T. Oishi, Org. Lett. 15 (2013) 2846–2849.